Journal of Inorganic Biochemistry 271 (2025) 112977

Contents lists available at ScienceDirect

Journal of Inorganic Biochemistry

journal homepage: www.elsevier.com/locate/jinorgbio

Targeting DNA mismatches with metal complexes☆

Natália Kolozsvári, Martin R. Gill *

Department of Chemistry, Faculty of Science and Engineering, Swansea University, Swansea, UK

ARTICLE INFO

Keywords:
Rhodium
Ruthenium
Platinum
Mismatch DNA
MMR-deficient cancer

ABSTRACT

DNA mismatches are non Watson-Crick base pairs that arise from errors during replication or are the result of DNA damage. Normally repaired by the mismatch mediated repair (MMR) pathway, in cancers deficient in MMR, such as subsets of colorectal and endometrial cancers, mismatches persist and accumulate, providing a biochemical vulnerability creating a target for small-molecule intervention. This review explores how metal complexes employing rhodium(III), ruthenium(II) or platinum(II) centres can exploit this molecular distinction to preferentially bind mismatch sites in DNA. We discuss the potential of this interaction to act as a foundation for next-generation therapeutics and imaging probes where the unique structural, electronic, and photophysical properties of metal complexes and associated ligand design offer opportunities to differentiate between canonical and mismatched DNA with high selectivity.

1. Introduction

1.1. Metal complexes and DNA

The design of metal complexes for DNA binding has demonstrated success in numerous applications ranging from therapeutic candidates to imaging and sensors [1,2]. Metal complexes have several advantageous properties in this capacity; features including tuneable ligand- or metal-centred reactivity, 3D molecular scaffolds distinct from pure organics, and access to partially filled d shells that provide suitability for redox, luminescence and electron transfer activities. Based on these criteria, numerous binding modes between metal complexes and DNA can be achieved, including direct coordination bond formation from the metal centre to the bases or backbone of DNA, sometimes referred to as "covalent" or "irreversible" binding, or non-bond forming associations such as within the grooves or between base pairs (metallo-intercalation), together categorised as "reversible" binding (reviewed in detail in [3]). Whilst molecules able to bind to canonical duplex DNA remain of relevance and are encountered in a diverse range of studies such as phosphorescent DNA dyes for light microscopy or novel anti-cancer candidates, it is arguably their ability to bind DNA in a structure- and sequence-specific manner that has attracted the greatest excitement for their potential within biology. As part of these efforts, targeting non-canonical DNA presents an opportunity to explore the chemistry and biology of diverse DNA structures to exploit the flexibility coordination chemistry provides (reviewed in [4–11]). The topic of this review is one such area: the ability of metal complexes to interact with DNA mismatches.

1.2. DNA mismatches

Mismatches (MM) are non-Watson Crick or "mismatch" base pairs, such as CC or GA. Mismatches in DNA occur when a non-complementary base pair is incorporated during replication, heteroduplex formation or as an effect of DNA-damaging ionising radiation or mutagenic chemicals [12]. Frequently, mismatches are inserted due to geometric variations of the DNA helix, or the tautomerisation of bases [13]. In cells, proofreading happens both during and after DNA synthesis; the latter utilising mismatch mediated repair (MMR), a DNA damage repair pathway that acts to preserve genomic stability [14]. Failure in mismatch repair – such as within MMR-deficient cells – leads to the accumulation of errors in the newly synthesised DNA strand. These errors are the mismatch base pairs themselves or the resultant microsatellites, short regions of repeated nucleotides.

1.2.1. MMR-deficient cancer

The loss of expression of an MMR protein and resultant microsatellite instability is a common genetic alteration in numerous cancers. One of the most common types of cancer caused by MMR-deficiency is Lynch Syndrome, or hereditary non-polyposis colorectal cancer (HNPCC),

☆ This article is part of a Special issue entitled: 'MetalsNon-Canonical DNA' published in Journal of Inorganic Biochemistry.

* Corresponding author.
E-mail address: m.r.gill@swansea.ac.uk (M.R. Gill).

https://doi.org/10.1016/j.jinorgbio.2025.112977
Received 1 May 2025; Received in revised form 27 May 2025; Accepted 16 June 2025
Available online 24 June 2025

patients of which have an increased chance of developing colorectal, endometrial and ovarian cancers [15]. MMR deficiency is present in approximately 15 % of all colorectal cancers and 30 % of endometrial cancers [16–20]. Moreover, research shows that mismatch repair deficiency in cancer cells is associated with increased resistance to some chemotherapeutics, such as platinum complexes, fluoropyrimidine compounds or methylating agents [21,22]. For this reason, devising treatments for these cell types is sorely needed. The structural differences between mismatch and canonical DNA provide opportunities to design small molecules that preferentially bind these structures, whilst the formation of mismatches in MMR-deficient cancers provides therapy and diagnostic opportunities.

Recent epidemiological data on MMR-deficient cancers has been analysed in a number of papers. A 2024 study of rectal cancer patients in the Netherlands revealed that MMR-status of the cancer was determined in 54.9 % of patients, 2.8 % of which proved to be MMR-deficient. Four years later the initial treatment outcomes were evaluated: while the local reoccurrence rate of MMR-deficient and MMR-proficient tumours were 4.7 % and 9.6 %, respectively, the overall survival rates were comparable between the two groups, 85.5 % and 82.2 % [23]. This finding is consistent with a 2022 report and systematic review by Swets et al, focusing on rectal cancers with microsatellite instability [24], as well as with a 2024 study by Justesen et al. [25] A 2025 report that analysed 66 studies across 11 different solid tumours reported a 20.5 %, 8.7 %, 8.2 % and 5.4 % prevalence of mutated MMR genes in endometrial, bladder, colorectal and gastroesophageal cancer respectively, noting that the included somatic MMR-mutation rate is lower than the overall MMR-deficiency reported in literature previously, which includes the epigenetic silencing of the genes as well. It was determined that mutation of the MMR genes has no significant effect on overall survival rate in most tumours, except for gastroesophageal cancer, in which case mutations correlate with increased survival [26].

1.2.2. *Mismatch frequency*

DNA replication is highly efficient, where DNA polymerase and base pair geometry are able to achieve an error rate of 10^{-4} to 10^{-5} during DNA synthesis [27]. In addition to this, a proofreading exonuclease can correct synthesis, resulting in an overall error rate of 10^{-7} per base pair (bp) per replication. The small frequency of errors that remain are then corrected by mismatch repair, further increasing the overall fidelity of DNA replication [28]. MMR efficiency can vary based on several factors, including the type of mismatch, its location in the genome and cell-cycle phase [29,30]. Quantitative studies in *Saccharomyces cerevisiae* demonstrate this efficiency: Lujan et al. stated that approximately one out of every 2000 replication forks will generate a mismatch for subsequent correction by MMR [31].

In MMR-deficient human cells, which would be expected to possess an elevated level of DNA mismatches, techniques generally quantify downstream genetic signatures, for example microsatellite instability or mutation frequency, to provide evidence of mismatch accumulation. For example, CRISPR modified human tumour cell organoids have provided evidence by way of mutation signatures that would be consistent with an ~2000-fold increase of DNA mismatches in MMR-deficient cells compared to MMR-proficient [32].

1.3. *Mismatch stability and structure*

Mismatches can be categorised as transition mismatches, when a purine and a pyrimidine base are paired, or transversion mismatches, with purine-purine and pyrimidine-pyrimidine mismatches (Fig. 1–2) [13]. As would be predicted based on deviation from preferred Watson-Crick pairing, the stability and structure of the DNA is affected by the inclusion of a mismatch [33–35]. An early study undertaken by Aboul-ela et al. in 1985 determined the cytosine-containing mismatches CC and CA to be the least thermodynamically stable, closely followed by CT, TT and AA [36]. The inclusion of guanine-containing mismatches, such as GG, GT and GA, were the least destabilising. This work also showed that oligomer stability additionally depends on the surrounding DNA sequence. A separate study by Song-Hua et al. examined longer, 373 bp DNA sequences differing in one base pair at one out of four possible sites, 48 DNAs in total, to evaluate the stability of mismatches in different base-stacking environments [37]. The study used temperature-gradient gel electrophoresis to separate the different strands by their melting points and confirmed C as the most destabilising base to be included in a mismatch. G was verified as the least destabilising base and revealed purine-purine mismatches to be generally more stable than pyrimidine-pyrimidine mismatches. Slight variations on the stability of the mismatches based on different neighbouring environments, such as the order of stability between GA, GT and GG mismatches changes depending on the location within the DNA strand. This study also determined the AA mismatch to be generally more or equally as stable as TT, and more stable than C-containing mismatches. Later studies reinforced these findings [38], and suggested that some mismatches destabilise the helix further than just the MM site: while GG, AA and TT destabilisations seem to be confined to the immediate vicinity, a CC mismatch has an effect up to 7–9 bp away [35].

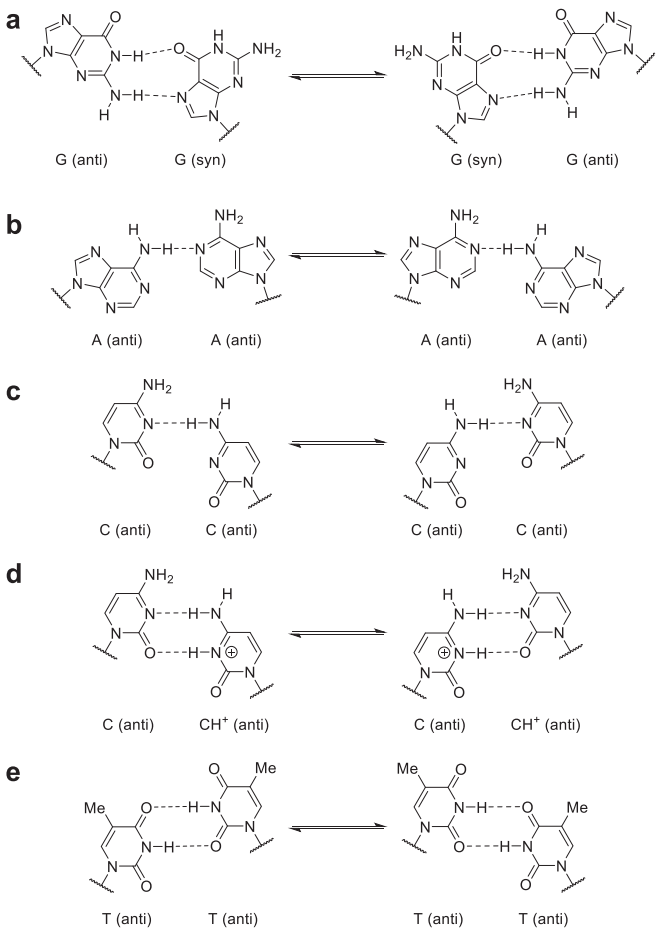

Fig. 1. Chemical structures of same-base mismatches: a. GG, *anti-syn* and *syn-anti* Hogsteen pairs, b. AA *anti-anti* wobble pairs, c. CC *anti-anti* wobble-like pairs, d. C-CH^+ *anti-anti* wobble pairs, e. TT *anti-anti* wobble pairs.

The quantified stability of different mismatches can be traced back to their hydrogen-bonding properties. Several studies have been conducted to determine the number of H-bonds between each mismatched base pair. Mismatched bases can pair in different conformations: while the Watson-Crick (WC) pairing (*anti-anti*) is most common for well-matched (WM) bases, mismatches also commonly take on WC-like properties. One such pair is GT [39], which is one of the most stable mispairings, stabilised by two H-bonds. Only the *anti-anti* conformation is associated

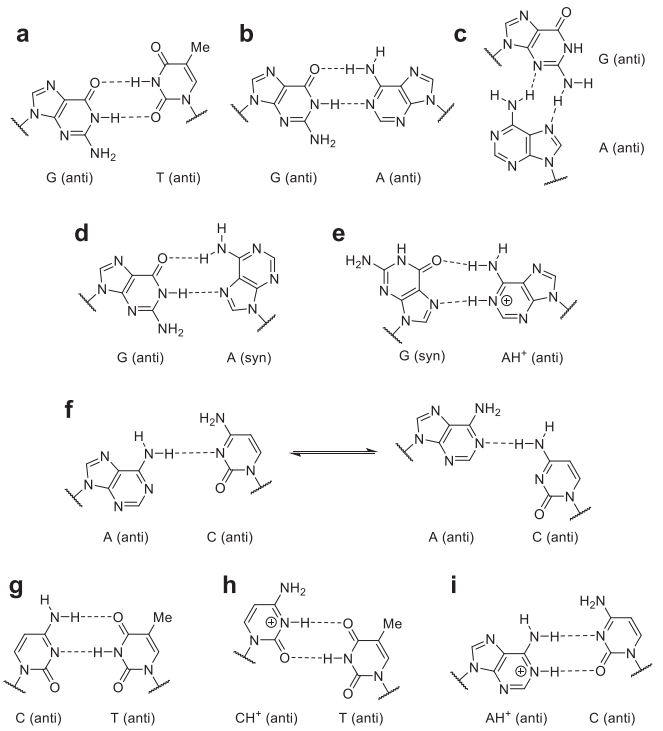

Fig. 2. Chemical structures of different-base mismatches: a. GT, *anti-anti* wobble pair, b. GA *anti-anti* pair, c. GA *anti-anti* sheared pair, d. GA *anti-syn* Hoogsteen pair, e. G-AH$^+$ *syn-anti* Hoogsteen pair, f. AC *anti-anti* wobble-inverted wobble pairs, g. CT *anti-anti* pair, h. CH$^+$-T *anti-anti* pair, i. AH$^+$-C *anti-anti* wobble pair.

with this pairing, however, large stacking interactions have been observed, indicating displacement of the bases compared to the canonical GC pair, resulting in a sheared, wobble-like pairing [40]. Hoogsteen pairs [41,42], or pairs in *syn-anti* or *anti-syn* conformation can also be found in DNA, predominantly in alternative DNA structures, such as triple helices [43,44] or G-quadruplexes [45]. They are characterised by one purine base rotating 180° around the glycosidic bond, thereby allowing previously inaccessible atoms to contribute to hydrogen bonding [46]. The GG purine-purine base pair is the most stable in this conformation, demonstrating double hydrogen bonding with either *anti-syn* or *syn-anti* pairing [47–49].

The last guanine-containing mismatch, GA, is among the most stable on account of the two hydrogen bonds between the two bases. This pairing can exist in several different conformations: standard Watson-Crick *anti-anti*, Hoogsteen *anti-syn* at neutral and basic pH, *syn-anti* below pH 5.5 with a protonated adenine, or in a sheared position stacked over each other, when tandem GA mismatches are present [50,51]. The AA purine-purine mismatch is strongly dependent on the flanking base pairs, and has been shown to have no H-bonding in some cases; however, it generally exists in *anti-anti* wobble pairs [52,53]. The AC mismatch is one of the least stable MM, as its conformation and hydrogen bonding is highly reliant on the environment. In acidic pH, the adenine takes on a protonated form, which can form a two-bond wobble pair with cytosine; however, the pair's neutral form is more unstable, only forming one H-bond and existing between a wobble and inverted wobble state [54,55].

While multiple nuclear magnetic resonance (NMR) and molecular dynamics (MD) studies have determined the CT mismatch to include two H-bonds at both neutral and C-protonated state [56,57], recent calculations have questioned this [58]. The pairing is among the most thermodynamically unstable and highly destabilises the DNA duplex with little variation depending on the neighbouring pairs. The stability of the TT mismatch has been determined to be roughly the same as the AA: it exists in interconverting *anti-anti* wobble conformation with two H-bonds stabilising the pair [52,59], although the exact bonding interactions depend on the surrounding bases [58]. Finally, the CC mismatch is reportedly the least thermodynamically stable out of the eight possible pairings [35,38]: although presenting in an interconverting wobble-like structure similar to TT, there is only one stabilising bond between the bases. In acidic environments, one cytosine quickly becomes protonated and they form a more stable wobble-like structure employing two hydrogen bonds [59].

Recently, Oliveira et al. attempted to characterise all different single, double and triple DNA mismatches in different next-nearest neighbour environments, 4032 different combinations in total [58]. They used the mesoscopic model, proposed by Peyrard and Bishop [60], from which hydrogen bonding and stacking interactions can be calculated. The amount/strength of hydrogen bonds are derived from the Morse potential: the higher the potential, the stronger the bonding interaction. This study proposed the thermodynamic stability of the mismatches as GA ≈ GT > GG > AG > TG > AA ≈ TT > AC ≈ TC > CA > CT > CC, which is in agreement with previous studies [33,35,38] in all but one instance: in the case of CT, consensus states two hydrogen bonds between the bases, while with this method, the low Morse potential alludes to weak hydrogen bonding interactions, the reasons of which are unclear.

Although DNA mismatches are thermodynamically destabilising, this does not necessarily mean major geometric conformation changes within the DNA strand. However, work has revealed that the presence of a mismatch can result in structural distortions of the DNA helix. For example, purine–purine mismatches often cause widening of the helix while pyrimidine–pyrimidine mismatches may cause narrowing [61]. However, purine-purine mismatches can also exhibit stacking with the opposing base, instead of with neighbouring bases; this can disrupt the normal B-form of the DNA [53].

In addition to this, structural studies have shown bending or kinking of DNA structure centred at the mismatch site, where it has been postulated that this flexibility is a key aspect required for recognition by mismatch repair proteins such as MutS in *E. coli* [62]. Other studies have provided evidence for reduced free energy for both bending [63] and base flipping [64] for DNA duplexes containing a mismatch compared to canonical matches. However, MD simulations of each mismatch base pair by Rossetti et al. did not show dramatic global alterations in the DNA duplex, and the authors suggested that specific DNA-protein interactions are needed to obtain such structures [65]. This study did show local changes in the DNA: the mismatches alter the twist angle, widen or narrow the major and minor grooves. Mismatches with higher breathing frequency, meaning the dynamics of the base pair, will cause more flexibility in the DNA helix. MM that are more readily recognised and corrected by DNA repair proteins were demonstrated to have higher breathing frequencies, such as GG, demonstrating 66 %, or AA 40 % breathing, while CC, a poorly repaired mismatch [66] only showed around 1 % breathing frequency, similar to well-matched base pairs, confirming local flexibility might be a factor for recognition by MMR proteins [67,68].

Johnson and Beese characterised all 12 mismatches at the primer terminus in the active site of a polymerase by X-ray crystallography; clearly demonstrating how mismatch-induced disruptions of the polymerase active site will stall replication [69]. Notably, these structures also demonstrated that the distortions extend beyond the mismatch itself, affecting the overall conformations of both the DNA and the protein at the active site. In agreement with this, Afek et al. provided evidence that mismatches increase transcription factor binding affinity and that this was the result of structural distortions generated [61]. This provides a mechanism by which a mismatch facilitates protein-DNA recognition to modulate its repair.

2. Targeting DNA mismatches with small molecules

2.1. Organic molecules

Although the primary focus of this review is metal complexes, various types of organic molecules have been discovered to selectively bind mismatches. The most researched compounds include macrocyclic bisintercalators, naphthyridine dimers and analogues, melamine-conjugates, groove-binders, small organic dyes and antibiotics (Fig. 3). This section will provide a brief summary of these mismatch-binders; for further information we direct readers to an excellent review on the topic by Granzhan et al. [70]

Macrocyclic bisintercalators employ two substituted naphthalene or anthracene moieties connected by aliphatic chains making a macrocycle. This flexibility allows them to intercalate at two sites at the same time, while threading around the groove. Bisnaphthalene macrocycles were shown to stabilise 17-mer duplex DNA through DNA melting experiments, where strands including a TX mismatch (TT, TC or TG) had a 9–11 °C increase in melting temperatures, while the well-matched sequence showed no stabilisation. Comparison with a non-macrocyclic bisnaphthalene derivative confirms that the connection between the naphthalene moieties is required for optimal selectivity. The anthracene moiety was proposed to enhance DNA-binding without discrimination due to increased π-stacking ability, however naphthalene compound, while weaker binders, showed more selectivity towards mismatches [71].

Macrocyclic bisintercalators have flexible chains between two aromatic regions, which allow them to both insert at the mismatch site and intercalate into a neighbouring area. These compounds tend to be more selective towards less thermodynamically stable mismatches, such as CC, TC, TT and abasic sites [71–73]. Other bisintercalator-like ligands, such as naphthyridine dimer (ND) analogues, can also recognise GG, GA and AA mismatches [74,75].

MMR-deficient cancer cell targeting using small molecule DNA mismatch-binders is a relatively new concept; therefore the amount of existing research is low [76]. In 2018, anticancer antibiotic echinomycin was found to exhibit preferential intercalation at TT mismatch sites, as well as a 2.7-times higher cytotoxicity in HCT116 MMR-deficient colorectal cancer cell line, compared to the MMR-restored HCT116 + Ch3 (IC_{50} or half inhibitory concentrations of 31.6 nM and 86.4 nM, respectively) [77]. The same group then screened the combination of echinomycin alongside actinomycin D, also an anti-cancer DNA intercalator, to bind DNA mismatches [78]. They found that cooperative intercalative binding of the two molecules was able to stabilise TT mismatches and X-ray analysis indicated distortion of individual DNA strands to a greater extent than well-matched DNA or single drug binding. In addition to this intriguing "co-selectivity", the drug combination was synergistic in MMR-deficient HCT116 cells and showed an encouraging anti-tumour effect in xenograft models.

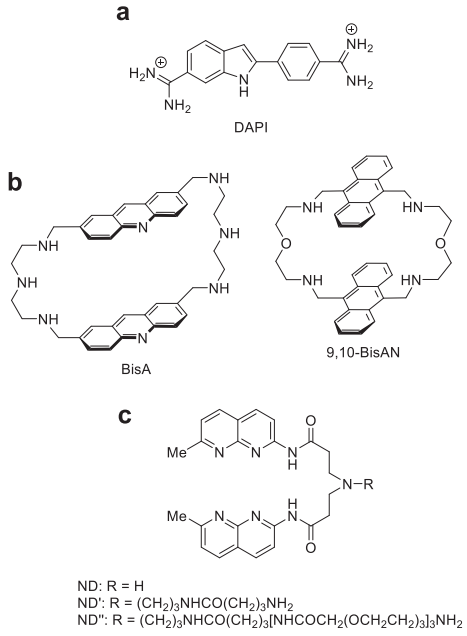

Fig. 3. Examples of organic mismatch interactive compounds: Organic minor-groove binder DAPI (a), macrocyclic bisintercalators (b) and bisintercalator-like ligands (c).

2.2. Metal complexes

2.2.1. Rhodium metallo-intercalators

One of the first metallo-intercalator targeting mismatches was [Rh(bpy)$_2$(chrysi)]$^{3+}$ (**1**) (bpy = 2,2′-bipyridine, chrysi = 5,6-chrysenequinone diimine) (Fig. 5a), discovered by the Barton group in 1997. While the chrysi ligand is too wide to easily intercalate into well-matched DNA, it can exploit the thermodynamic destabilisation of mismatched base pairs. This complex has a higher affinity to the less stable pyrimidine-pyrimidine mismatches, which was demonstrated in photocleavage experiments [79]. The complex recognises mismatches with 80 % selectivity and even can detect them in linear DNA containing up to 2725 base pairs [80].

Several analogous rhodium complexes were also investigated for their mismatch-binding ability, including cyclometalated [Rh(ppy)$_2$(chrysi)]$^{+}$ (**2**) (ppy = 2-phenylpyridine) (Fig. 4b), which, while it has an affinity to CC mismatches, shows a 14-fold decrease in binding strength compared to **1** [81].

[Rh(bpy)$_2$(phzi)]$^{3+}$ (**3**) (phzi = benzo[*a*]phenazine-5,6-quinone diimine) (Fig. 4a) was developed as a bulkier alternative to the chrysi ligand. It has a binding constant two orders of magnitude higher than its parent complex, due to the greater π-π stacking ability of the phzi ligand. The mismatch selectivity also remained unchanged, targeting primarily CC, TC and TT mismatches [82]. The biological activity of **1** and **3** was investigated in an experiment with MMR-proficient and MMR-deficient HCT116 human colon cancer, and Msh2^{+}/Msh2^{-} mouse fibroblast cell lines. In both experiments, the rhodium complexes preferentially inhibited the cell proliferation of the MMR-deficient cell lines. Compared to DNA-methylating agent *N*-methyl-*N*′-nitro-*N*-nitrosoguanidine (MNNG), which is more cytotoxic to MMR-proficient cell lines, this provides a difference to most common chemotherapeutics. Irradiation of the cells after the incubation period produced even greater inhibition of cell proliferation in the MMR-deficient cell line treated with Δ-**1** [83].

The cytotoxicity of **1**, [Rh(HDPA)$_2$(chrysi)]$^{3+}$ (**4**) and [Rh(MeDPA)$_2$(chrysi)]$^{3+}$ (**5**) (HDPA = 2,2′-dipyridylamine, MeDPA = *N*-methyl-2,2′-dipyridylamine) (Fig. 5a) was also tested in MTT cytotoxicity assay with previous MMR-proficient and MMR-deficient HCT116 cells. The two complexes are reported to have selective cytotoxicity towards MMR-deficient cells (Fig. 5b), and flow cytometry showed that

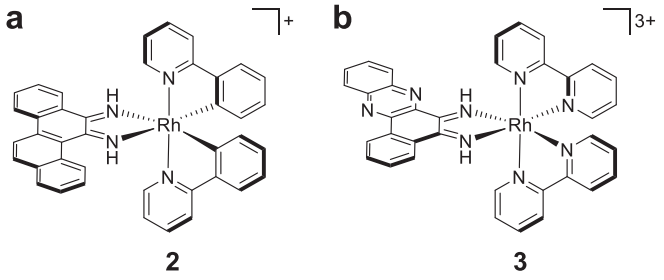

Fig. 4. Structures of [Rh(ppy)$_2$(chrysi)]$^{+}$ (**2**) (a) and [Rh(bpy)$_2$(phzi)]$^{3+}$ (**3**) (b).

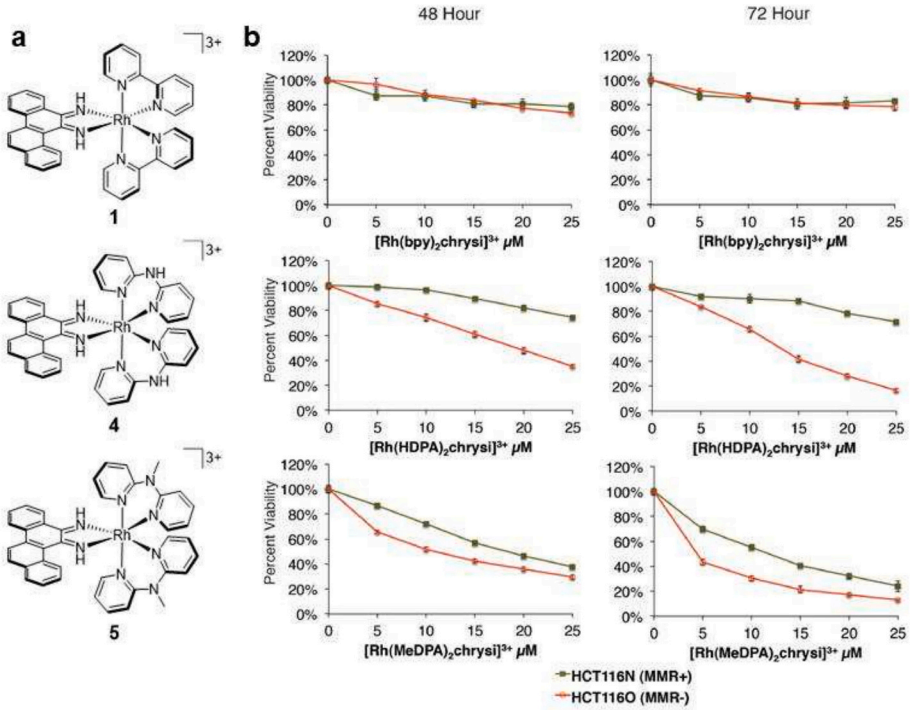

Fig. 5. a. Structures of $[Rh(bpy)_2(chrysi)]^{3+}$ (**1**), $[Rh(HDPA)_2(chrysi)]^{3+}$ (**4**) and $[Rh(MeDPA)_2(chrysi)]^{3+}$ (**5**). b. Cytotoxicity of the three Rh complexes towards the MMR-deficient HCT116O and MMR-proficient HCT116N cell lines. Reprinted with permission from reference [84]. Copyright 2011, American Chemical Society.

the cell cycle is disrupted before cell death [84].

A complex employing three different ligands, $[Rh(chrysi)(phen)(PPO)]^{2+}$ (**6**) (RhPPO, PPO = 2-(pyridine-2-yl)propan-2-ol, phen = 1,10-phenanthroline) (Fig. 6a) was found to have a 100-times greater cell potency than earlier rhodium complexes. It demonstrated cytotoxicity towards MMR-deficient cells in HCT116, as well as lung and ovarian cancer cell lines. It was proved to inhibit DNA transcription and synthesis, as well as blocking cell-cycle progression by generating a lesion in the DNA which activates the DNA damage response [85]. The complex was also tested in 27 colorectal cancer cell lines. It is confirmed to be on average 5-times, and in some cases 100-times more potent than cisplatin. It is moderately selective towards MMR-deficient cell lines; however, cellular uptake is lower in these cells, therefore making this selectivity less pronounced [86].

As an effort to develop a rhodium complex with luminescent properties, a Cyanine-3 (Cy3) dye was conjugated to $[Rh(phen)(chrysi)(HDPA)]^{3+}$ (**7**) with a polyethylene glycol (PEG) linker, resulting in RhCy3 (**8**) (Fig. 6b) [87]. This complex has low luminescence in aqueous solutions and with well-matched DNA sequences, however when bound to the CC mismatch, luminescence increases 9-fold (Fig. 6c). Fluorescence titrations determined the binding affinity to 27-mer DNA with a CC mismatch to be $K_B(CC) = 3.1 \times 10^6\ M^{-1}$, a similar value to other Rh complexes, such as parent complex **7** ($K_B(CC) = 2.3 \times 10^6\ M^{-1}$) [88].

The Barton group used **8** to confirm the preferential cytotoxicity of **6** towards MMR-deficient cell lines [86]. The genomic DNA of eight cancer cell lines was extracted and luminescence titrations of **8** were performed. Apart from one outlier cell line with two MMR-genes missing compared to only one in the other MMR-deficient cell lines, a strong correlation was found between the IC_{50} concentrations demonstrated by **6** and the **8** luminescence: IC_{50} was lower, and luminescence higher in cell lines with MMR-deficiency (Fig. 6d), confirming the genomic DNA and most importantly, DNA defects as the target for this complex.

To further develop luminescent Rh probes, a second generation was introduced, with the Cy3 dye attached directly to **6**, by leaving the PPO ligand unmodified [89]. The new complex, RhPPO-Cy3 (**9**) (Fig. 7a), had comparable DNA-binding to the parent complex ($K_B(CC) = 1.8 \times 10^6\ M^{-1}$ and $5.4 \times 10^6\ M^{-1}$, respectively). The luminescent complex was tested against HCT116O MMR-deficient and HCT116N MMR-proficient cell lines, and the half maximal effective concentration or EC_{50} against the former proved to be around half of the latter (1.0 ± 0.1 μM and 1.9 ± 0.2 μM, respectively) over 72 h of treatment, demonstrating selectivity towards the MMR-deficient cell line. The complex was shown to localise in the nucleus; nuclear foci were present in the HCT116O cells, suggesting selectivity based on DNA mismatches (Fig. 7b). DNA damage induced by the complex was evaluated by phospho-H2AX marking, which was consistent with the Cy3 staining results. The presence of the complex does not trigger the apoptotic pathway where instead cells underwent necrotic cell death.

The cellular distribution of rhodium metalloinsertors was tested with $[Rh(DPAE)_2chrysi]^{3+}$ (**10**) (DPAE = 2-(di(pyridine-2-yl)amino)ethanol) and $[Rh(PrDPA)_2chrysi]^{3+}$ (**11**) (PrDPA = N-propyl-N-(pyridin-2-yl) pyridin-2-amine) (Fig. 8). These complexes primarily differ in their lipophilicity due to the substitution on their ancillary ligands, with logP = −1.5 and − 1.0 values, respectively. Both are excellent DNA mismatch-binders, **10** demonstrating a slightly higher affinity towards CC mismatches. Their cellular uptake was tested in HCT116O cells over 24 h, in which 4.3-times more **11** was found to accumulate in cells compared to **10**. Their subcellular localisation was tested by inductively coupled plasma mass spectrometry (ICP-MS), and equal concentrations of both complexes were found in the nucleus; however, this is only attributed to the higher uptake of **11**. When looking at distribution by ICP-MS, around 75 % of the more hydrophilic **10** localised in the nucleus, compared to only 30 % of **11**, which was predominantly attracted to the mitochondria instead. This confirms that while lipophilicity might help the uptake of complexes into the cells, if the nucleus or DNA is the intended target, more hydrophilic complexes could be more effective [90,91].

2.2.2. *Ruthenium metallo-intercalators*

Based on their ability to emit from long-lifetime MLCT (metal-to-ligand charge transfer) states, ruthenium(II) polypyridyl complexes (RPCs) have shown significant potential as DNA probes and cellular

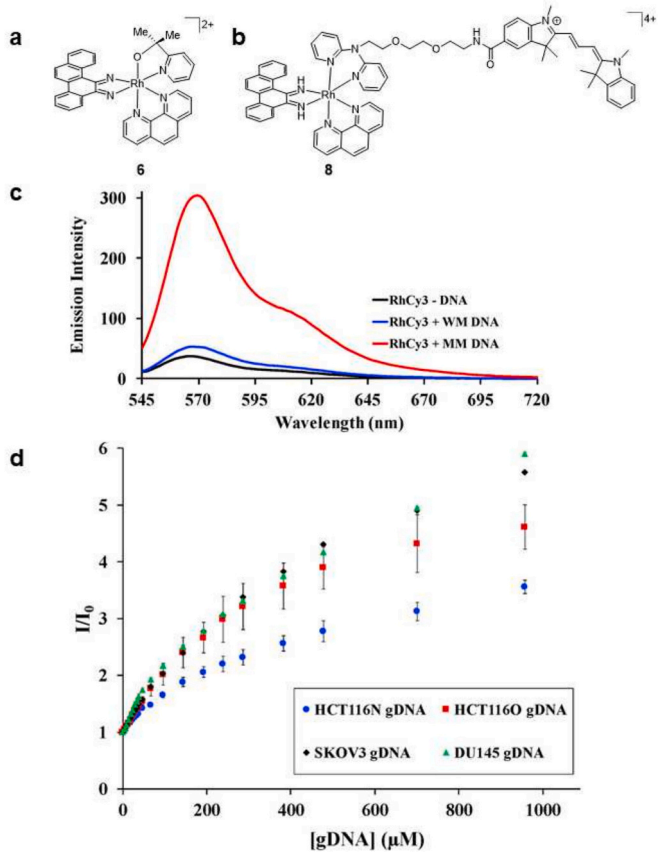

Fig. 6. Structure of a. RhPPO (**6**) and b. RhCy3 (**8**). c. Emission intensity of **8** bound to well-matched, CC-mismatched or no DNA. d. Fluorescence titrations of **8** with genomic DNA extracted from MMR-proficient HCT116N or MMR-deficient HCT116O, SKOV3 or DU145 cell lines. Reprinted with permission from reference [87]. Copyright 2017 American Chemical Society.

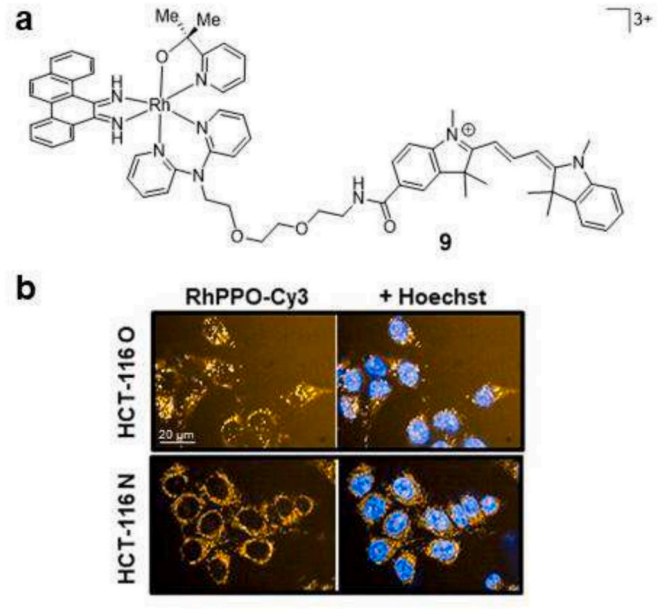

Fig. 7. a. The chemical structure of RhPPO-Cy3 (**9**). b. Nuclear foci of **9** in MMR-deficient HCT116O cells, and the absence in MMR-proficient HCT116N cells, demonstrating mismatch-specific DNA binding in genomic DNA. Reprinted with permission from reference [89]. Copyright 2020, American Chemical Society.

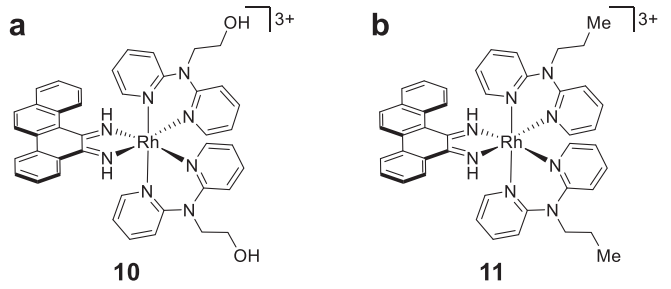

Fig. 8. The chemical structures of a. $[Rh(DPAE)_2chrysi]^{3+}$ (**10**) and b. $[Rh(PrDPA)_2chrysi]^{3+}$ (**11**).

DNA imaging agents [92]. In cells, ruthenium(II) metallo-intercalators that achieve sufficient nuclear uptake act to stall DNA replication forks [93] and generate altered anti-cancer activity profiles compared to current DNA-damaging agents, including in cisplatin-resistant cell lines [94,95].

The Barton group investigated ruthenium(II) complexes in parallel to rhodium(III) complexes for mismatch selectivity. $[Ru(bpy)_2(dppz)]^{2+}$ (**12**) (dppz = dipyrido[3,2-a:2′,3′-c]phenazine) (Fig. 9a), as well as being a DNA light-switch complex [96], can distinguish between well-matched and mismatched DNA. The complex shows a 1.5-fold increase in luminescence when bound to CC-mismatch or abasic site-containing oligonucleotides. This is different from other common luminescent DNA-probes, like ethidium bromide, which shows little difference when bound to WM or MM DNA. The complex also shows preference towards other, thermodynamically less stable mismatches, such as AA and AC, while showing no difference when intercalated into GG, GT and GA-containing sequences (Fig. 9b). Surprisingly, the luminescence does not increase in the presence of TT and CT mismatches, despite each of these mismatches having similar stability to AA and AC [97]. This could be due to hydrogen bonding interactions between the dppz ligand of the complex and the thymine in the base pair [98].

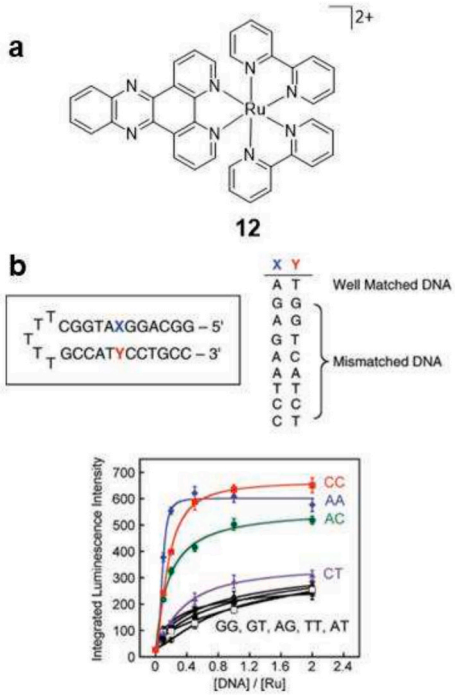

Fig. 9. a. Structure of $[Ru(bpy)_2dppz]^{2+}$ (**12**). b. Luminescence titrations of **12** with hairpin DNA containing a well-matched or mismatched base pair in place of XY. Reprinted with permission from reference [98]. Copyright 2009 American Chemical Society.

The crystal structure of Δ-**12** bound to a DNA oligonucleotide containing two AA mismatches was presented by Song et al. [99] It was determined that the complex binds to mismatch sites by metalloinsertion, ejecting the two adenine bases from the helix, while at well-matched sites, intercalation occurs. The luminescence of the complex was found to be three times higher when bound to the mismatched oligomer compared to the well matched one, and upon addition of minor groove quencher $[Cu(phen)_2]^{2+}$, its luminescence was quenched by 34 % in case of MM, and only 12 % in case of WM sequence, which demonstrates minor groove binding at mismatch, and major groove binding at the well-matched sites.

Derivatives of **12** with bulkier intercalating ligands have been developed and tested, with the aim of combining the mismatch selectivity of rhodium(III) complexes with the luminescent properties of ruthenium(II) complexes. Phenanthroline-containing functional group ligands were employed, such as pqp (6-phenylquino[8,7-k][1,8]phenanthroline), tpqp (7,8,13,14-tetrahydro-6-phenylquino[8,7-k][1,8] phenanthroline) and tactp (4,5,9,18-tetraazachryseno[9,10-b]-triphenylene) [100], as well as chrysi, previously used in rhodium complexes, and its analogues [101]. The chrysi ligand and analogues displayed no or weak luminescent properties, therefore were not good candidates as "light-switch" complexes, despite demonstrating mismatch selectivity [70,101]. Phenanthroline derivatives, while displaying luminescence, had different problems. While there is evidence that some of them do bind at the mismatch site, $[Ru(bpy)_2(tpqp)]^{2+}$ shows no increase in luminescence when bound to DNA, and $[Ru(bpy)_2(tactp)]^{2+}$ forms aggregates in aqueous solutions, which makes it more difficult to draw conclusions from DNA titrations [100].

In 2015, two phenanthroline-based RPCs were developed, $[Ru(bpy)_2furphen]^{2+}$ (**13**) and $[Ru(bpy)_2imiphen]^{2+}$ (**14**) (furphen = 2-(furan-2-yl)-1*H*-imidazo[4,5-*f*][1,10]phenanthroline and imiphen = 2-(1*H*-imidazol-2-yl)-1*H*-imidazo[4,5-*f*][1,10]phenanthroline), with low DNA-binding constants [102]. While the affinity to DNA is not extraordinary, both complexes exhibit an ~5-times enhanced luminescence in the presence of well-matched DNA, and 1.2–1.5-fold selectivity towards CC mismatches quantified by luminescence measurements. The complexes did not show any selectivity towards different mismatches or abasic sites.

$[Ru(Me_4phen)_2(dppz)]^{2+}$ (**15**) (Me_4phen = 3,4,7,8-tetramethyl-1,10-phenanthroline) (Fig. 10a) has similar luminescent properties to **12**, albeit at a substantially reduced emission intensity. Despite this, it is able to act as a DNA "light-switch" like its parent compound, however, it can reportedly distinguish between WM and MM DNA. Its luminescence was measured while binding to DNA hairpins with different WM and MM base pairs in the middle. It demonstrated an approximately 6-fold increase when bound to CC mismatches, and preferential binding towards CA, TT and CT mismatches as well (Fig. 10c) [103].

DNA titrations with WM and MM 27-mer DNA oligomers were also performed (Fig. 10d). The complex showed a far greater luminescence when bound to the mismatch, opposed to the GC match, and was calculated to have a 26-fold increase in binding affinity. Comparing results between **15** and **12** indicates the success of the relatively simple strategy of increasing steric bulk of ancillary ligands to reduce canonical DNA affinity, resulting in greater selectivity for mismatch sites.

As seen with rhodium complexes, bulkier functional group ligands have been employed to develop complexes with improved mismatch selectivity. $[Ru(bpy)_2(BNIQ)]^{2+}$ (**16**) (BNIQ = benzo[c][1,7]naphthyridine-1-isoquinoline) (Fig. 10b) contains the sterically demanding BNIQ ligand, which preserves the luminescent properties of the complex. Titrations were performed with 27-mer DNA containing either a GC match, CC mismatch or an abasic site. The emission intensities were approximately 1.5-fold higher for the mismatched or abasic site-containing DNAs, with an about 500-fold increase in the value of the binding constants [104].

"Elbow-shaped" ruthenium complexes (Fig. 11) have also been investigated for their DNA-binding properties. Out of all the complexes studied by Deraedt and Marcélis, $[Ru(bpy)_2(bdppz)]^{2+}$ (**17**) (bdppz = benzo[*h*]dipyrido[3,2-a:2′,3′-c]phenazine) demonstrates a maximum of 3.5-fold increase in luminescence intensities when bound to mismatched hairpin oligonucleotides compared to their well-matched counterparts [105].

Gillard et al. tested acridine-based Ru(II) complexes $[Ru(phen)_2(dpac)]^{2+}$ (**18**) (dpac = dipyrido[3,2-*a*:2′,3′-*c*]acridine), a Ru-dppz analogue, as well as the elbow-shaped $[Ru(bpy)_2(npp)]^{2+}$ (**19**)

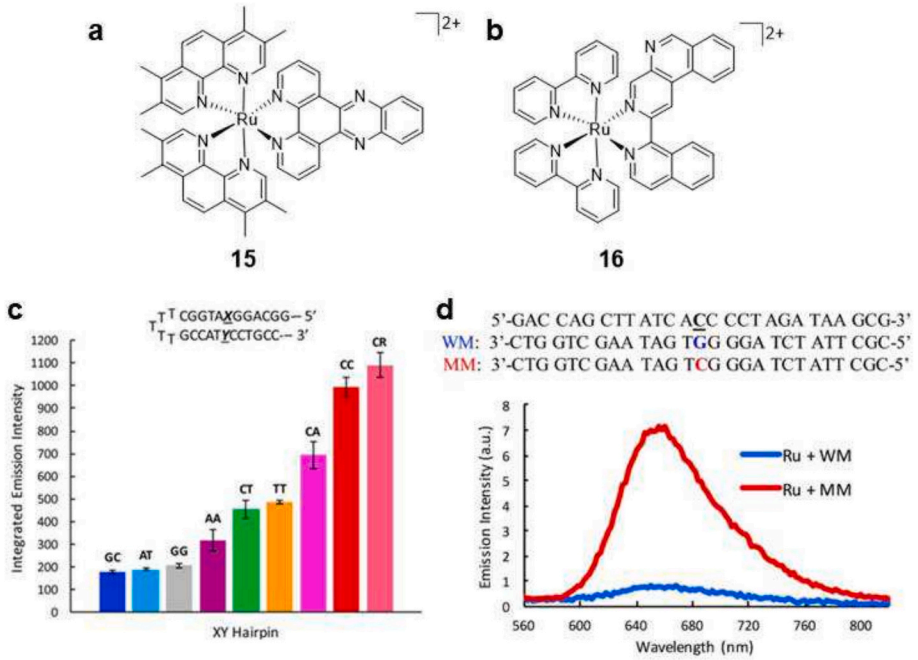

Fig. 10. Structure of $[Ru(Me_4phen)_2dppz]^{2+}$ (**15**) (a) and $[Ru(bpy)_2(BNIQ)]^{2+}$ (**16**) (b). c. Emission intensity of **15** bound to different hairpin DNAs. d. DNA titration of **15** with well-matched and mismatched 27-mer DNA oligomers. Figures reprinted with permission from reference [103]. Copyright 2016 American Chemical Society.

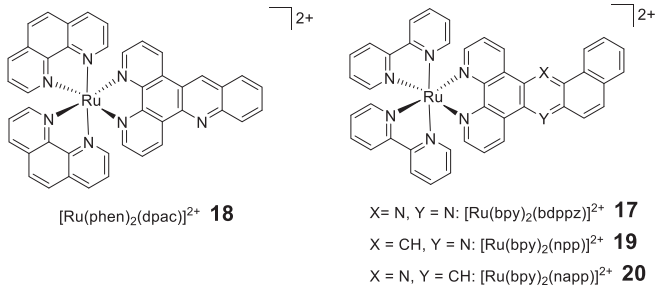

Fig. 11. Chemical structure of ruthenium(II) complexes $[Ru(phen)_2(dpac)]^{2+}$ (**18**), $[Ru(bpy)_2(bdppz)]^{2+}$ (**17**), $[Ru(bpy)_2(npp)]^{2+}$ (**19**) and $[Ru(bpy)_2(napp)]^{2+}$ (**20**).

(npp = naphtho[1,2-*b*]pyrido[3,2-f][1,7]phenanthroline) and $[Ru(bpy)_2(napp)]^{2+}$ (**20**) (napp = naphtho[2,1-*b*]pyrido[3,2-*f*][1,7]phenanthroline) for their DNA-binding affinities (Fig. 11). All three complexes displayed increased luminescence when bound to DNA, and when mismatch-selectivity was tested, they all demonstrated brighter luminescence bound to well-matched sites. While **18** was not able to distinguish between the types of mismatches [99], **19** and **20** were, with the latter demonstrating superior differentiation [105,106].

The Cardin group has been focusing their work on X-ray crystallographic images of ruthenium complexes bound to DNA [107]. While a lot of their work focuses on well-matched sequences [108–111], recently rac-$[Ru(phen)_2phi]^{2+}$ (**21**) (phi = 9,10-phenanthrenediimine) (Fig. 12a) was crystallised with 12-mer DNA sequence $d(CGCTATAATGCG)_2$ containing two TT-AA double mismatch sites (Fig. 12) [112]. The crystal structure showed a largely kinked DNA structure with Λ-**21** bound at the mismatch site, as well as several of the mismatched bases flipped out of the helix or shifted to a new position to accommodate the complex, allowing them to pair with the appropriate base (Fig. 12b). The "flipped out" bases also demonstrate H-bonding interactions with the complex, stabilising the interaction. It was determined that the complex is not intercalated or inserted, but essentially encapsulated in the bulge the adenosine created. The Δ-enantiomer of the complex is also present in the structure, however with no interaction with the bases, instead stacking with the Λ-complex and being enveloped by the oligomer.

In terms of cellular activity, as far as we are aware, relatively few RPCs have been investigated in an MMR context to date. First, the aforementioned **15** showed preferential cytotoxicity towards HTC116O MMR-deficient human colorectal cancer cell line compared to the MMR-proficient HTC116N. Mechanistic investigation was not attempted and so the basis for cytotoxicity, and role of DNA targeting, is unknown [103]. Secondly, the bis-ruthenium $[^{111}In][In\{Ru(tpm)(dppz)\}_2((pyCH_2NH)_2DTPA)]^{4+}$ (**22**) (tpm = tris-(1-pyrazolyl)methane, DTPA = diethylenetriaminepentaacetic acid) (Fig. 13a) complex was reported by Gill et al. The indium-labelled complex demonstrated higher binding affinity to CT-DNA than the unlabelled counterpart, and while it did not show preferential binding to mismatches in hairpin DNA, it did reveal a significant preference towards TT mismatches in 10-mer oligonucleotides, both with increased luminescence and the stabilisation of the sequence in thermal denaturation studies (Fig. 13b). Successful nuclear targeting was demonstrated by both confocal microscopy (Fig. 13c) and measured radioactivity in fractionated cells. These results also indicated that the nuclei of DLD-1 colorectal cancer cells had an especially high concentration of the complex. When radiotoxicity was compared in DLD-1 MMR-deficient and DLD-1 + Chr2 MMR-restored cell lines, DLD-1 cells demonstrated significantly diminished survival (Fig. 13d). As no inherent difference in radiosensitivity to external beam γ-ray ionising radiation between cell lines was observed, this confirmed selective targeting of MMR-deficient cells with a targeted radionuclide therapeutic [113].

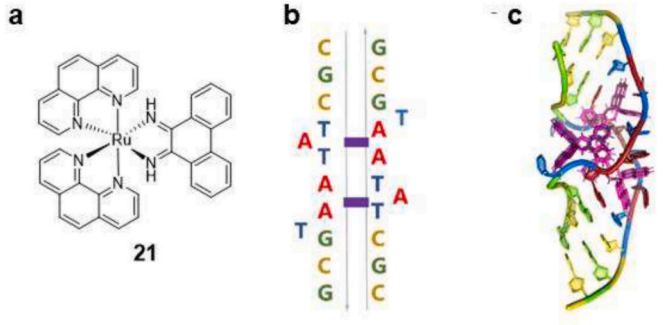

Fig. 12. a. Structure of $[Ru(phen)_2phi]^{2+}$ (**21**). b. Ejection and re-pairing of bases upon the binding of **21**. c. The structure and kinking of $d(CGCTATAATGCG)_2$ oligomer with two molecules of the complex bound at the mismatch sites. Reprinted from reference [112], with permission from the Royal Society of Chemistry.

Finally, our group recently utilised the ability of MLCT emissive RPCs to undergo Förster resonance energy transfer (FRET) with Cyanine 5.5-labelled (Cy5.5) DNA to show two complexes bind CC mismatches in 27mer DNA (Fig. 14) [114]. This novel FRET assay determines RPC-Cy5.5 proximity which, in turn, can provide evidence that the mismatch site itself is being targeted by the complexes. Employing this method, $[Ru(5,5\text{-dmb})_2(dppz)]^{2+}$ (**23**) and $[Ru(dppz)_2(5,5'\text{-dmb})]^{2+}$ (**24**) (5,5′-dmb = 5,5′-dimethyl-2,2′-bipyridine) were identified as a CC mismatch-interactive complexes, with derived K_d values indicating a mild selectivity. The result for **23** supported a previous observation by Boynton et al. [99]. Complexes were tested in a small panel of cell lines, and whilst activities were reasonable – including evidence of impacting DNA replication as provided by DNA fibre assay – no enhanced cytotoxicity towards MMR-deficient HCT116 colorectal carcinoma cells was found. One weakness in this study is that a paired cell line was not employed to elucidate the precise role of MMR status in the observed activity profiles.

2.2.3. *Platinum complexes*

Platinum drugs such as cisplatin are widely used chemotherapeutics employed for the treatment of various tumour types [115]. The major target of cisplatin is DNA, where platinum-DNA adducts interfere with multiple cellular processes to block cell replication and generate a variety of forms of DNA damage. However, MMR status is linked to cisplatin sensitivity, where MMR pathway proteins have been shown to be essential to maintain a cisplatin sensitive phenotype [116]. The basis of this is that MMR proteins are able to recognise cisplatin-DNA adducts and block their repair, thereby resulting in increased DNA repair in MMR-deficient cells [117]. An additional factor is presented by the essential role certain MMR proteins play in triggering apoptosis in response to DNA damage induced by cisplatin [118]. In either case, or the combination of both, cisplatin resistance in MMR-deficient cancer cell results [119]. Based on this understanding, although designing sequence-specific Pt(II) irreversible binders is certainly achievable [120], it would not be predicted that mismatch-interactive Pt(II) cisplatin derivatives would be good candidates to reverse cisplatin resistance in MMR-deficient cells.

Reversible binding holds more promise and square planar Pt(II) complexes have long been viewed of interest as potential therapeutics (see [121] and references within). An additional benefit is that cyclometallated Pt(II) pincer complexes can demonstrate intense, long lifetime luminescence courtesy of $^3\pi - \pi^*$ transitions [122]. With this in mind, and considering work tailoring Rh(III) and Ru(II) complexes for mismatches outlined above, Fung et al. designed a series of $[Pt^{II}(C\hat{}N\hat{}N)(NHC)]^+$ (**25**) (NHC = N-heterocyclic carbene) (Fig. 15a) complexes with varying steric bulk of the NHC group [123]. They found that an increase of steric hindrance of the NHC ligand resulted in decreased matched DNA binding, however, interaction with CC mismatched DNA remained high. This resulted in the isolation of complexes that show up

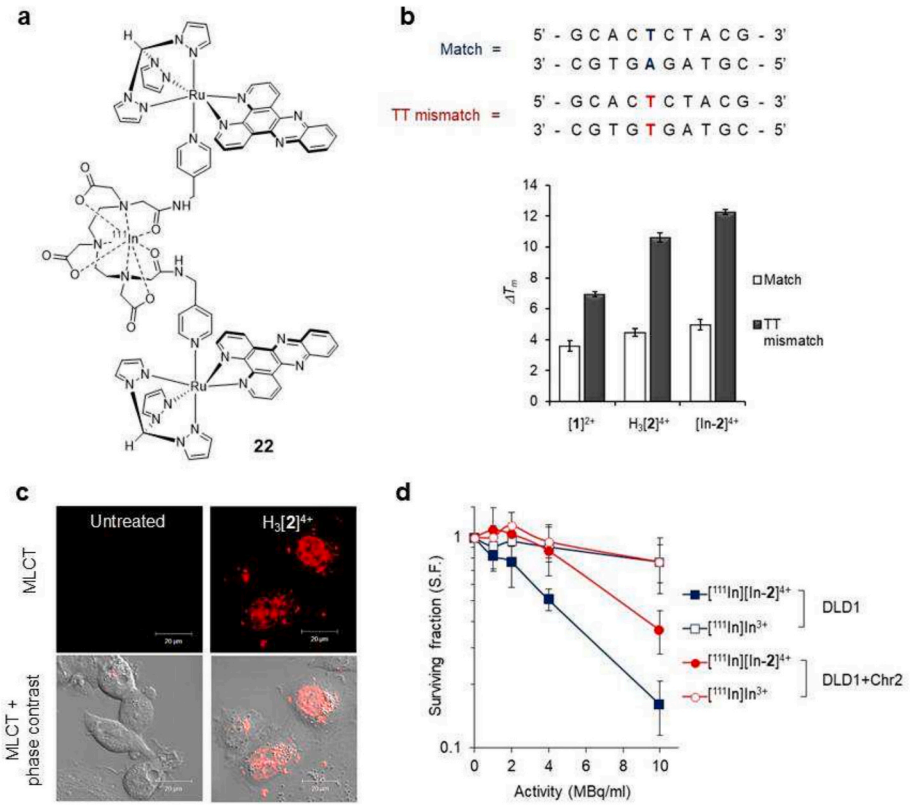

Fig. 13. a. Structure of $[^{111}In][In\{Ru(tpm)(dppz)\}_2((pyCH_2NH)_2DTPA)]^{4+}$ (**22**) b. Thermal denaturation studies showing increased ΔT_m for a 10-mer containing a single TT mismatch site compared to well matched. c. Confocal laser scanning micrograph of HCT116 cells showing nuclear MLCT emission of Ru(II) scaffold. d. Radiotoxicity towards DLD-1 (MMR-deficient) or DLD-1 + Chr2 (MMR-restored) human colorectal cancer cell lines, as determined by clonogenic survival assay. Results adapted from reference [113].

to 15-fold higher emission intensities upon binding to mismatched DNA over matched DNA (Fig. 15b). For more thermodynamically stable mismatches than CC, a dinuclear Pt(II) complex linked by a bridging diphosphine ligand (**26**) was employed (Fig. 15a). This had a reduced (6-fold) difference in luminescence sensitivity, however, a greater binding affinity to CC mismatches was described. Moreover, **26** showed higher emission in the presence of other mismatches compared to matched DNA, acting to justify their synthetic strategy. In permeabilised cells, a stronger emission signal was seen in MMR-deficient HCT116 cells compared to HCT116N cells. However, one deficiency of the study was lipophilic Pt(II) complexes accumulating in lysosomes in live cells, which restricted further biological evaluation.

A related study was presented by Gabbr and Pigge, who synthesised a series of cyclometalated platinum(II) complexes with sterically expansive tetraarylethylene ligands (**30**) (Fig. 16a) and examined the ability of these complexes to interact with well-matched and mismatched hairpin oligonucleotides [124]. They found that increased steric bulk of the tetraarylethylene ligands resulted in greater luminescence in the presence of a mismatch-containing hairpin versus well-matched (Fig. 16b). Similar to Fung et al., the greatest enhancement was a 14-fold increase in the presence of the CC-containing sequence. DNA melting confirmed preferential stabilisation of the CC-containing hairpin over well-matched while luminescence quenching experiments were consistent with metalloinsertion as a binding mode.

3. Future directions and conclusions

To date, there have been no clinical trials for a small molecule specifically designed to target DNA mismatches; however, this review illustrates the progress made in developing molecules selective for these non-canonical DNA structures and, in some cases, evidence of preferential activity towards MMR-deficient cancer cell lines (summarised in Table 1). Work on isolating mismatch-interactive metal complexes has shown coordination chemistry to have many advantages in this capacity. First, the ability to utilise a scaffold to independently design a mismatch-interactive ligand and select ancillary ligands to reduce the affinity to native duplex DNA. Second, selection of a functional metal centre, such as for photocleavage or electron transfer at the mismatch site. Third, employing Ru(II) polypyridyl or Pt(II) cyclometallated chemistry provides access to long-lived MLCT or $^3\pi - \pi^*$ luminescence that can quickly assess selectivity and function as imaging agents towards mismatch-containing DNA sequences. Fourth: Molecules can be designed for multi-functionality, for example mismatch-interactive binding centres can be conjugated to a fluorescent dye or even therapeutic radionuclide. Finally, access to DNA binding modes such as metallo-intercalation or metallo-insertion that can achieve distinct cellular responses compared to existing DNA damaging drugs.

It is also the case that challenges remain, the largest of which remains selectivity combined with apparent infrequency of mismatches, even in MMR-deficient cells (the "needles in a basestack" conundrum as described by Granzhan et al. [70]). As such, even exquisitely designed molecules that have a substantially increased binding affinity for mismatch sites may encounter binding competition with well-matched DNA, as these latter sequences will vastly outnumber mismatches within the genome. However, considering that binding modality clearly plays a substantive role in biological response, achieving altered binding at mismatches compared to canonical duplex DNA potentially represents the biggest advance within this area. For this reason, the demonstration by the Barton group that metallo-insertion only at mismatch sites occurs is significant. Given the substantial structural distortions to native DNA induced by intercalation and metallo-intercalation—and the consequential cellular responses—compared to the minimal perturbation

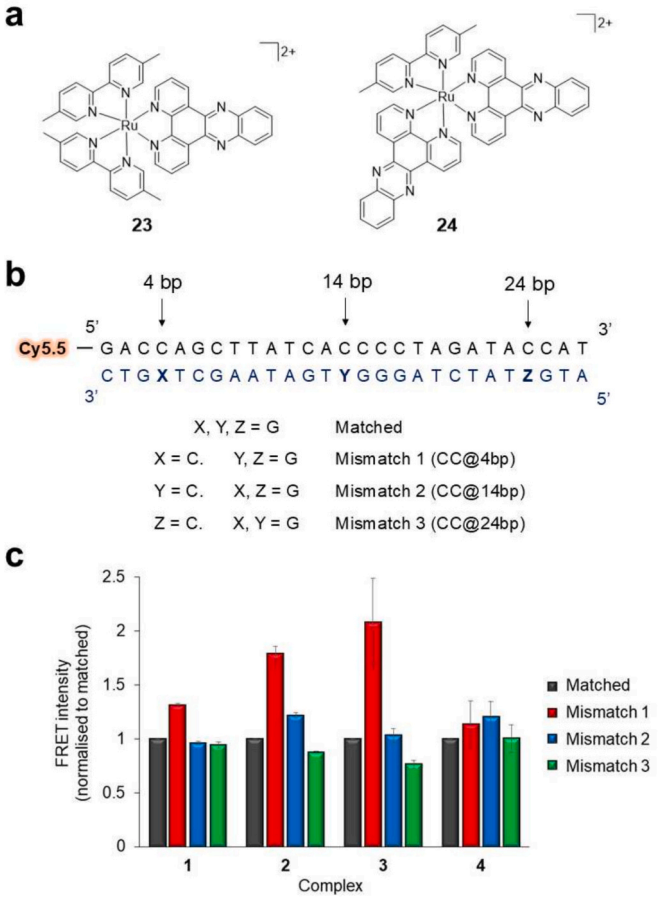

Fig. 14. a. Structures of $[Ru(5,5\text{-dmb})_2(dppz)]^{2+}$ (**23**) and $[Ru(dppz)_2(5,5'\text{-dmb})]^{2+}$ (**24**). b. Matched and mismatch-containing Cy5.5-labelled 27-mer DNA duplexes where the CC mismatch is located at 4, 14 and 24 bp from Cy5.5 label. c. FRET intensity of Ru(II) complexes with the addition of Cy5.5-labelled 27-mer duplexes. For complexes **23** and **24**, FRET intensity is proportional to Cy5.5-CC distance. Figure adapted from reference [114].

caused by groove-binding, the design of switchable DNA-binding molecules that selectively adopt an intercalative mode at mismatched sites could represent a promising strategy to enhance selectivity for MMR-deficient cells. Other lines of future enquiry could be combination of a mismatch-interactive molecule with external stimuli. For example, transition metal complexes are well-known to act as photosensitizers (Ru(II) and Ir(III)) [125] and radiosensitizers (Pt(II), Ru(II), Au) [126], achieving synergistic cytotoxicity with light and high-energy ionising radiation, respectively. In both cases, DNA damage may be generated either directly or indirectly (via reactive oxygen species or ROS). It would therefore be useful to examine whether highly localised DNA damage could be facilitated at - or in close proximity to - the mismatch site. This would have the potential to achieve high selectivity as it would be based upon both the presence of a target (mismatches) and the external stimuli, which can be focussed on specific regions or even cells. Similarly, use of synergistic drug combinations of DNA targeting metal complexes with DNA damage response inhibitors such as Olaparib can achieve high potency in aggressive cancer classes such as triple negative breast cancer [127–129]. It would be fascinating examining whether a mismatch selective molecule could achieve similar results with improved selectivity in MMR-deficient cancers.

Despite the success employing octahedral Rh(III) and Ru(II) scaffolds, it is also the case that relatively few metal centres have been utilised to date. Examination of a greater number of cyclometallated Pt (II) systems would add to the encouraging early work mentioned within this review. As such systems interact with DNA by reversible binding

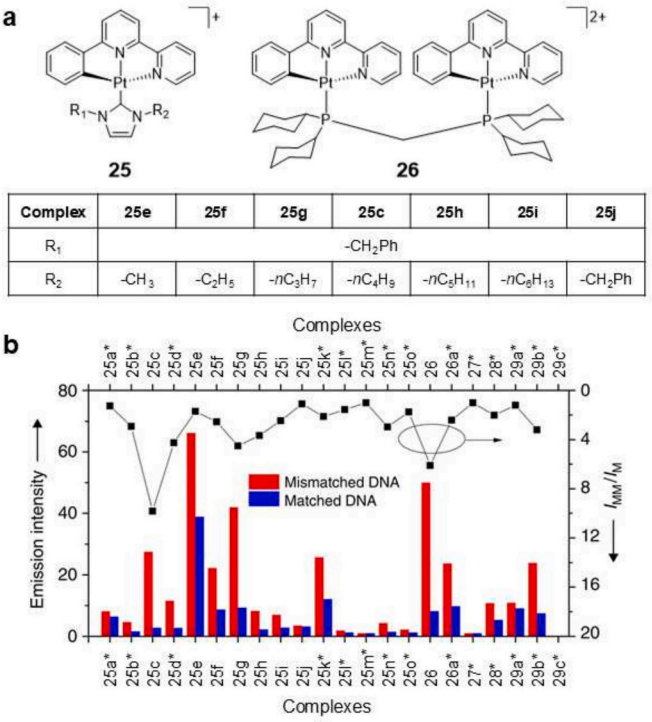

Fig. 15. a. Structure of mononuclear $[Pt^{II}(C\hat{}N\hat{}N)(NHC)]^{+}$ complexes (**25**) and dinuclear $[Pt^{II}_2(C\hat{}N\hat{}N)_2(\mu\text{-dcpm})]^{2+}$ complex (**26**). b. Emission intensity of luminescent platinum complexes upon the addition of well-matched or CC-mismatched hairpin DNA. The bar chart represents the emission intensity, the scatter plot the relative intensity of MM to WM strand. The complex numbers labelled with * are outside the scope of this review. Reprinted with permission from reference [123]. Copyright 2016, The Authors.

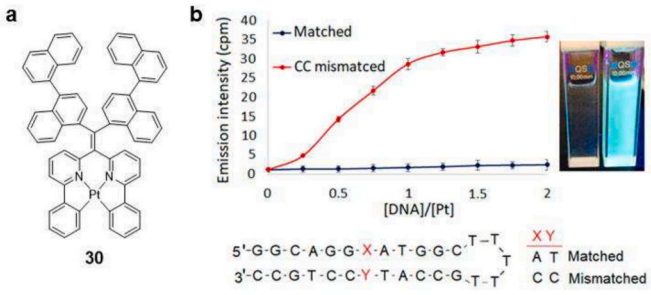

Fig. 16. a. The chemical structure of a Pt(II) complex employing tetraarylethylene ligands (**30**). b. Emission intensity of luminescent platinum complex **30** upon the addition of well-matched or CC-mismatched hairpin DNA. The solutions placed under UV light are depicted to the right side of the figure: well-matched sequence to the left, mismatched sequence on the right. Reprinted with permission from reference [124]. Copyright 2018, American Chemical Society.

modalities rather than direct platination, altered DNA damage responses to cisplatin and derivatives may be generated in a manner analogous to that observed for Ru(II) intercalators. Due to the role MMR proteins play in repair of cisplatin-induced DNA damage, and the corresponding link between MMR-deficiency and cisplatin resistance, it is feasible that such non-canonical DNA damage could offer an altered profile of activity compared to conventional platinum therapeutics and retain activity in MMR-deficient cells. However, greater investigation into the precise DNA damage response initiated in response to DNA damage in cells - particularly the role of MMR proteins in their repair – by Pt(II) and Ru (II) DNA metallo-intercalators or metallo-insertors would be required to better explore this concept. Examining work on gold complexes in

Table 1
Comparative table of mentioned rhodium, ruthenium and platinum complexes, their DNA- and mismatch-binding affinity, cytotoxicity, MMR-selectivity and mechanism of action, where applicable.

Complex	K_b (CT-DNA) (M^{-1})	Mismatch selectivity	Cytotoxicity		Cell line selectivity	Mechanistic endpoints
			Cell line	IC_{50} (μM)		
1 [79,80,83,84]	–	$K_b = 3.4 \times 10^7$ M^{-1} (CC, 29-mer DNA hairpin) $K_b = 2.2 \times 10^6$ M^{-1} (CA, 29-mer DNA hairpin)	–	–	No significant toxicity, selectivity or preferential DNA synthesis inhibition in HCT116O and HCT116N cell lines in 48 h, selectivity towards HCT116O at 96 h	–
3 [82]	–	$K_b = 3.0 \times 10^6$ (CA, 31-mer DNA) $K_b = 1 \times 10^7$ (CC, 31-mer DNA) $K_b = 6 \times 10^7$ (CT, 31-mer DNA)	–	–	Decreased DNA synthesis in MMR-deficient *Msh2*- mouse fibroblasts compared to *Msh2*+ control; preferential inhibition of HCT116O MMR-deficient compared to HCT116N MMR-proficient cell line (96 h)	Able to differentiate genomic DNA based on MMR-status of cell line by photocleavage
4 [84]	–	$K_b = 2.0 \times 10^7$ M^{-1} (CC, 29-mer DNA hairpin) $K_b = 2.6 \times 10^6$ M^{-1} (AC, 29-mer DNA hairpin)	–	–	More cytotoxic towards the MMR-deficient HCT116O compared to HCT116N (MMR-proficient)	Decrease in S-phase population in cell cycle, increase in G1- and G2/M-phase, slightly more pronounced in HCT116O cells; selective cell death (necrosis) in HCT116O
5 [84]	–	–	–	–	More cytotoxic towards the MMR-deficient HCT116O compared to HCT116N (MMR-proficient)	–
6 [85,86]	–	$K_b = 5.5 \times 10^6$ M^{-1} (CC, 36-mer DNA)	HCT116O	0.15 ± 0.06 (EC_{50}, 72 h)	7.5× selectivity towards MMR-deficient cell line	Inhibition of cell division and DNA transcription, accumulation of DNA damage, cell cycle arrest in G2/M phase, non-apoptotic cell death in MMR-deficient cells
			HCT116N	1.12 ± 0.27 (EC_{50}, 72 h)		
8 [86,87]	–	9.0× (CC) $K_b = 3.1 \times 10^6$ M^{-1} (CC, 27-mer DNA)	–	–	–	Able to differentiate genomic DNA based on MMR-status of cell line
9 [89]		$K_b = 1.8 \times 10^6$ M^{-1} (CC, 27-mer DNA)	HCT116O	1.0 ± 0.1 (EC_{50}, 72 h)	1.9× selectivity towards MMR-deficient cell line	Direct DNA damage, necrosis
			HCT116N	1.9 ± 0.2 (EC_{50}, 72 h)		
10 [88–91]	–	$K_b = 6.8 \times 10^6 M^{-1}$ (CC, 29-mer DNA hairpin) nano	–	–	–	Inhibition of cell growth in HCT116O MMR-deficient cells
11 [88–91]	–	$K_b = 2.5 \times 10^6 M^{-1}$ (CC, 29-mer DNA hairpin)	–	–	–	Mild loss of cell viability in HCT116O MMR-deficient cells
12 [98]	$>1.0 \times 10^6$ (absorbance)	1.5× (CC, abasic)	–	–	–	–
13 [102]	$6.7 \pm 0.2 \times 10^3$ (absorbance)	1.5× (CC)	–	–	–	–
14 [102]	$4.9 \pm 0.2 \times 10^4$ (absorbance)	1.2× (CC)	–	–	–	–
15 [103]	–	5.7× (CC), 6.3× (abasic)	–	–	Greater cytotoxicity towards HCT116O MMR-deficient cell line compared to HCT116N (MMR-proficient)	–
16 [104]	–	1.5× (CC, abasic)	–	–	–	–
17 [105]	6.86×10^5 (luminescence)	3.5× (CC)	–	–	–	–
18 [106]	4.16×10^5 (luminescence)	2.0× (multiple)	–	–	–	–
19 [105,106]	8.31×10^4 (luminescence)	1.6× decrease (CT), 1.3× decrease (CC)	–	–	–	–
20 [113]	1.00×10^5 (luminescence)	3.0× decrease (TT)	–	–	–	–
22 [113]	$1.1 \pm 0.2 \times 10^6$ (luminescence)	1.7× (TT)	HCT116 (colorectal)	34 (72 h)	Greater radiotoxicity towards DLD-1 and HCT116 MMR-deficient cell line compared	DNA damage, γH2AX expression in MMR-deficient cell lines

(*continued on next page*)

Table 1 (*continued*)

Complex	K_b (CT-DNA) (M^{-1})	Mismatch selectivity	Cytotoxicity		Cell line selectivity	Mechanistic endpoints
			Cell line	IC_{50} (μM)		
			HeLa (cervical)	32 (72 h)	to DLD-1 + Chr2 and HT-29 (MMR-proficient)	
23 [114]	2.632×10^6 (luminescence)	–	MDA-MB-231 (breast)	>100 (72 h)	More selective towards certain cancer cell lines, no selectivity towards MMR-deficiency	–
			HCC38 (breast)	>100 (72 h)		
			HCT116 (colorectal)	53.7 ± 9.9 (72 h)		
			T24 (bladder)	34.4 ± 3.3 (72 h)		
			MCF10A (normal epithelial)	>100 (72 h)		
24 [114]	1.248×10^6 (luminescence)	–	MDA-MB-231 (breast)	21.8 ± 2.9 (72 h)	More selective towards cancer cell lines, no selectivity towards MMR-deficiency	Synergy with PARP inhibitor Olaparib
			HCC38 (breast)	3.8 ± 2.5 (72 h)		
			HCT116 (colorectal)	16.4 ± 1.4 (72 h)		
			T24 (bladder)	28.0 ± 4.4 (72 h)		
			MCF10A (normal epithelial)	>100 (72 h)		
25 [123]	–	10.2× (CC)	–	–	–	–
26 [123]	–	6.1× (CC)	–	–	Significantly stronger emission from HCT116 MMR-deficient cells (permeabilised) than HCT116N (MMR-proficient)	–
30 [124]	–	14.3× (CC)	–	–	–	–

medicinal chemistry [130], Au(III) macrocyclic complexes containing pyrrolic fragments, organometallic Au(III)-N-heterocyclic carbenes or Au(III) pyridyl and isoquinolylamido complexes all have the ability to intercalate DNA and are highly tuneable via ligand modification. Development of these scaffolds for mismatch selectivity in a similar manner as for Pt(II) complexes would therefore increase the range of mismatch-interactive metal complexes and also provide a new avenue of exploration for gold therapeutics. Numerous Cu(II) complexes utilising polypyridyl ligands have been designed for DNA binding [131], and so use of mismatch-interactive ligands described in this review coordinated to a Cu(II) centre could prove useful. Cu(II) complexes are often efficient DNA cleaving agents and so this would then provide the ability to achieve localised DNA damage in close proximity to a mismatch. In a similar manner, Zn(II) and Ni(II) complexes would also be of interest, where similar binding affinities to the analogous Cu(II) complex are observed [132]. Not restricting work to small molecule complexes, supramolecular chemistry can also be employed for the selective recognition of non-canonical DNA [133]. For example, Zhu et al., developed a self-assembled supramolecular $FeII_4L_4$ tetrahedron cage able to interact with a range of DNA structures, including mismatch DNA base pairs [134]. Another example is provided by Pramanik et al., who showed that tripeptide-functionalized luminescent copper nanoclusters were able to recognise DNA containing a single base pair mismatch from well-matched sequences. Of particular significance is that binding was via a groove-binding interaction, thereby demonstrating that such selectivity can be achieved through a non-intercalative or insertion binding mode [135].

Finally, although the vast majority of work to date has utilised DNA, there has been increased attention drawn to RNA as a target in medicinal chemistry in recent years [136]. RNA can also contain mismatches in their secondary structure [137] and this can influence a diverse range of properties, including folding, tertiary structure, stability, protein-RNA interaction and viral replication [138–141]. Considering that mismatch interactive organic compounds have been examined in their capacity to bind RNA mismatches (see [142] and references within), the possibility of translating work on DNA mismatch interactive metal complexes to RNA in a similar manner is appealing. This would have significance in terms of expanding the range of final disease applications beyond cancer.

CRediT authorship contribution statement

Natália Kolozsvári: Writing – review & editing, Writing – original draft. **Martin R. Gill:** Writing – review & editing, Supervision, Funding acquisition.

Declaration of competing interest

The authors declare that they have no known competing financial interests or personal relationships that could have appeared to influence the work reported in this paper.

Acknowledgements

This work was supported by Cancer Research Wales (Pritchard and Moore Scholarship, grant no. 2542).

Data availability

No data was used for the research described in the article.

References

[1] C.X. Zhang, S.J. Lippard, New metal complexes as potential therapeutics, Curr. Opin. Chem. Biol. 7 (2003) 481–489, https://doi.org/10.1016/S1367-5931(03)00081-4.
[2] J. Berrones Reyes, M.K. Kuimova, R. Vilar, Metal complexes as optical probes for DNA sensing and imaging, Curr. Opin. Chem. Biol. 61 (2021) 179–190, https://doi.org/10.1016/j.cbpa.2021.02.007.
[3] B.J. Pages, D.L. Ang, E.P. Wright, J.R. Aldrich-Wright, Metal complex interactions with DNA, Dalton Trans. 44 (2015) 3505–3526, https://doi.org/10.1039/C4DT02700K.
[4] B.M. Zeglis, V.C. Pierre, J.K. Barton, Metallo-intercalators and metallo-insertors, Chem. Commun. (2007) 4565–4579, https://doi.org/10.1039/b710949k.

[5] C. Metcalfe, J.A. Thomas, Kinetically inert transition metal complexes that reversibly bind to DNA, Chem. Soc. Rev. 32 (2003) 215–224, https://doi.org/10.1039/b201945k.
[6] G.-Y. Li, R.-L. Guan, L.-N. Ji, H. Chao, DNA condensation induced by metal complexes, Coord. Chem. Rev. 281 (2014) 100–113, https://doi.org/10.1016/j.ccr.2014.09.005.
[7] A.M. Pizarro, P.J. Sadler, Unusual DNA binding modes for metal anticancer complexes, Biochimie 91 (2009) 1198–1211, https://doi.org/10.1016/j.biochi.2009.03.017.
[8] S. Georgiades, N. Abd Karim, K. Suntharalingam, R. Vilar, Interaction of metal complexes with G-quadruplex DNA, Angew. Chem. Int. Ed. 49 (2010) 4020–4034, https://doi.org/10.1002/anie.200906363.
[9] H.-K. Liu, P.J. Sadler, Metal complexes as DNA intercalators, Acc. Chem. Res. 44 (2011) 349–359, https://doi.org/10.1021/ar100140e.
[10] A.C. Komor, J.K. Barton, The path for metal complexes to a DNA target, Chem. Commun. 49 (2013) 3617–3630, https://doi.org/10.1039/c3cc00177f.
[11] P.D. Dayanidhi, V.G. Vaidyanathan, Structural insights into the recognition of DNA defects by small molecules, Dalton Trans. 50 (2021) 5691–5712, https://doi.org/10.1039/D0DT04289G.
[12] G. Rossetti, P.D. Dans, I. Gomez-Pinto, I. Ivani, C. Gonzalez, M. Orozco, The structural impact of DNA mismatches, Nucleic Acids Res. 43 (2015) 4309, https://doi.org/10.1093/NAR/GKV254.
[13] P. Modrich, DNA mismatch correction, Annu. Rev. Biochem. 56 (1987) 435–466, https://doi.org/10.1146/annurev.bi.56.070187.002251.
[14] M.F. Goodman, S. Creighton, L.B. Bloom, J. Petruska, Biochemical basis of DNA replication fidelity, Crit. Rev. Biochem. Mol. Biol. 28 (1993) 83–126, https://doi.org/10.3109/10409239309086792.
[15] D. Guillotin, S.A. Martin, Exploiting DNA mismatch repair deficiency as a therapeutic strategy, Exp. Cell Res. 329 (2014) 110–115, https://doi.org/10.1016/j.yexcr.2014.07.004.
[16] F.A. Sinicrope, DNA mismatch repair and adjuvant chemotherapy in sporadic colon cancer, Nat. Rev. Clin. Oncol. 7 (2010) 174–177, https://doi.org/10.1038/nrclinonc.2009.235.
[17] M.C. Olave, R.P. Graham, Mismatch repair deficiency: the what, how and why it is important, Genes Chromosom. Cancer 61 (2022) 314–321, https://doi.org/10.1002/gcc.23015.
[18] E. Fountzilas, T. Papadopoulos, E. Papadopoulou, C. Gouedard, H.P. Kourea, P. Constantoulakis, C. Magkou, M. Sfakianaki, V. Kotoula, D. Bantouna, G. Raptou, A.A. Saetta, G. Christopoulou, D. Hatzibougias, E. Michalopoulou-Manoloutsiou, E. Siatra, E. Eleftheriadis, E. Kavoura, L. Kaklamanis, A. Sourla, G. Papaxoinis, K. Pavlakis, P. Hytiroglou, C. Vourlakou, P. Arapantoni-Dadioti, S. Murray, G. Nasioulas, G. Timologos, G. Fountzilas, Z. Saridaki, Nationwide real-world data of microsatellite instability and/or mismatch repair deficiency in cancer: prevalence and testing patterns, Diagnostics 14 (2024) 1076, https://doi.org/10.3390/diagnostics14111076.
[19] R. Dorantes-Heredia, D. Motola-Kuba, I. Escamilla-López, E. Téllez-Bernal, E. Conde-Flores, D. Escalera-Santamaría, E. Medina-Ceballos, J. Ruiz-Morales, E. Dorokhova, L.E. Flores-García, G. Lugo, G. Del C. Filio-Rodríguez, Prevalence of mismatch repair deficiency in advanced solid tumors (colorectal cancer and non-colorectal cancer) in One Mexican Institution, J. Pers. Med. 14 (2024), https://doi.org/10.3390/jpm14121152.
[20] M. Lorenzi, M. Amonkar, J. Zhang, S. Mehta, K.L. Liaw, Epidemiology of microsatellite instability high (MSI-H) and deficient mismatch repair (dMMR) in solid tumors: a structured literature review, J. Oncol. 2020 (2020) 807929, https://doi.org/10.1155/2020/1807929.
[21] M. Hewish, C.J. Lord, S.A. Martin, D. Cunningham, A. Ashworth, Mismatch repair deficient colorectal cancer in the era of personalized treatment, Nat. Rev. Clin. Oncol. 7 (2010) 197–208, https://doi.org/10.1038/nrclinonc.2010.18.
[22] D. Guillotin, S.A. Martin, Exploiting DNA mismatch repair deficiency as a therapeutic strategy, Exp. Cell Res. 329 (2014) 110–115, https://doi.org/10.1016/j.yexcr.2014.07.004.
[23] E.G.M. van Geffen, C.R.C. Hogewoning, S.M.J.A. Hazen, T.C. Sluckin, M. M. Lange, P. Snaebjornsson, R.G.H. Beets-Tan, C.A.M. Marijnen, C. Verhoef, M. Chalabi, P.J. Tanis, M. Kusters, T.S. Aukema, Incidence and outcomes of patients with mismatch repair deficient rectal cancer operated in 2016: a Nationwide cohort from the Netherlands, Clin. Colorectal Cancer (2024), https://doi.org/10.1016/j.clcc.2024.12.003.
[24] M. Swets, C. Graham Martinez, S. van Vliet, A. van Tilburg, H. Gelderblom, C.A. M. Marijnen, C.J.H. van de Velde, I.D. Nagtegaal, Microsatellite instability in rectal cancer: what does it mean? A study of two randomized trials and a systematic review of the literature, Histopathology 81 (2022) 352–362, https://doi.org/10.1111/his.14710.
[25] T.F. Justesen, A. Orhan, A.W. Rosen, M. Gögenur, I. Gögenur, Mismatch repair status and surgical outcomes in localized colorectal cancer: a nationwide cohort study, Ann. Surg. Open 5 (2024) e499, https://doi.org/10.1097/AS9.0000000000000499.
[26] K. Venetis, C. Frascarelli, L.B. Bielo, G. Cursano, R. Adorisio, M. Ivanova, E. Mane, V. Peruzzo, A. Concardi, M. Negrelli, M. D'Ercole, F.M. Porta, Y. Zhan, A. Marra, D. Trapani, C. Criscitiello, G. Curigliano, E. Guerini-Rocco, N. Fusco, Mismatch repair (MMR) and microsatellite instability (MSI) phenotypes across solid tumors: a comprehensive cBioPortal study on prevalence and prognostic impact, Eur. J. Cancer 217 (2025), https://doi.org/10.1016/j.ejca.2025.115233.
[27] R.R. Iyer, A. Pluciennik, V. Burdett, P.L. Modrich, DNA mismatch repair: functions and mechanisms, Chem. Rev. 106 (2005) 302–323, https://doi.org/10.1021/cr0404794.
[28] A. Umar, T.A. Kunkel, DNA-replication fidelity, mismatch repair and genome instability in cancer cells, Eur. J. Biochem. 238 (1996) 297–307, https://doi.org/10.1111/j.1432-1033.1996.0297z.x.
[29] J.D. Hawk, L. Stefanovic, J.C. Boyer, T.D. Petes, R.A. Farber, Variation in efficiency of DNA mismatch repair at different sites in the yeast genome, Proc. Natl. Acad. Sci. 102 (2005) 8639–8643, https://doi.org/10.1073/pnas.0503415102.
[30] M.A. Edelbrock, S. Kaliyaperumal, K.J. Williams, DNA mismatch repair efficiency and fidelity are elevated during DNA synthesis in human cells, Mutat. Res. Fundam. Mol. Mech. Mutagen. 662 (2009) 59–66, https://doi.org/10.1016/j.mrfmmm.2008.12.006.
[31] S.A. Lujan, A.R. Clausen, A.B. Clark, H.K. MacAlpine, D.M. MacAlpine, E.P. Malc, P.A. Mieczkowski, A.B. Burkholder, D.C. Fargo, D.A. Gordenin, T.A. Kunkel, Heterogeneous polymerase fidelity and mismatch repair bias genome variation and composition, Genome Res. 24 (2014) 1751–1764, https://doi.org/10.1101/gr.178335.114.
[32] J. Drost, R. van Boxtel, F. Blokzijl, T. Mizutani, N. Sasaki, V. Sasselli, J. de Ligt, S. Behjati, J.E. Grolleman, T. van Wezel, S. Nik-Zainal, R.P. Kuiper, E. Cuppen, H. Clevers, Use of CRISPR-modified human stem cell organoids to study the origin of mutational signatures in cancer, Science 358 (2017) 234–238, https://doi.org/10.1126/science.aao3130.
[33] H.T. Allawi, J. Santalucia, Nearest-neighbor thermodynamics of internal A·C mismatches in DNA: sequence dependence and pH effects, Biochemistry 37 (1998) 9435–9444, https://doi.org/10.1021/bi9803729.
[34] H.T. Allawi, J. Santalucia, Thermodynamics and NMR of internal G·T mismatches in DNA, Biochemistry 36 (1997) 10581–10594, https://doi.org/10.1021/bi962590c.
[35] A. Tikhomirova, I. Beletskaya, T. Chalikian, Stability of DNA duplexes containing GG, CC, AA, and TT mismatches, Biochemistry 45 (2006) 10563–10571, https://doi.org/10.1021/bi060304j.
[36] F. Aboul-ela, D. Koh, I. Tinoco, F.H. Martin, Base-base mismatches. Thermodynamics of double helix formation for dCA3XA3G + dCT3YT3G (X, Y = A,C,G,T), Nucleic Acids Res. 13 (1985) 4811–4824, https://doi.org/10.1093/nar/13.13.4811.
[37] S.-H. Ke, R.M. Wartell, Influence of nearest neighbor sequence on the stability of base pair mismatches in long DNA: determination by temperature-gradient gel electrophoresis, Nucleic Acids Res. 21 (1993) 5137–5143, https://doi.org/10.1093/nar/21.22.5137.
[38] N. Peyret, P.A. Seneviratne, H.T. Allawi, J. SantaLucia, Nearest-neighbor thermodynamics and NMR of DNA sequences with internal A·A, C·C, G·G, and T·T mismatches, Biochemistry 38 (1999) 3468–3477, https://doi.org/10.1021/bi9825091.
[39] I.J. Kimsey, K. Petzold, B. Sathyamoorthy, Z.W. Stein, H.M. Al-Hashimi, Visualizing transient Watson-Crick-like mispairs in DNA and RNA duplexes, Nature 519 (2015) 315–320, https://doi.org/10.1038/nature14227.
[40] R.J. Isaacs, H.P. Spielmann, Insight into G-T mismatch recognition using molecular dynamics with time-averaged restraints derived from NMR spectroscopy, J. Am. Chem. Soc. 126 (2004) 583–590, https://doi.org/10.1021/ja037333r.
[41] K. Hoogsteen, The structure of crystals containing a hydrogen-bonded complex of 1-methylthymine and 9-methyladenine, Acta Crystallogr. 12 (1959) 822–823, https://doi.org/10.1107/S0365110X59002389.
[42] E.N. Nikolova, E. Kim, A.A. Wise, P.J. O'Brien, I. Andricioaei, H.M. Al-Hashimi, Transient Hoogsteen base pairs in canonical duplex DNA, Nature 470 (2011) 498–504, https://doi.org/10.1038/nature09775.
[43] P.A. Beal, P.B. Dervan, Second structural motif for recognition of DNA by oligonucleotide-directed triple-helix formation, Science 251 (1991) (1979) 1360–1363, https://doi.org/10.1126/science.2003222.
[44] J.-L. Mergny, J.-S. Sun, M. Rougée, T. Montenay-Garestier, F. Barcelo, J. Chomilier, C. Héléne, Sequence specificity in triple-helix formation: experimental and theoretical studies of the effect of mismatches on triplex stability, Biochemistry 30 (1991) 9791–9798, https://doi.org/10.1021/bi00104a031.
[45] J.E. Johnson, J.S. Smith, M.L. Kozak, F.B. Johnson, In vivo veritas: using yeast to probe the biological functions of G-quadruplexes, Biochimie 90 (2008) 1250–1263, https://doi.org/10.1016/j.biochi.2008.02.013.
[46] R.R. Sinden, Introduction to the structure, properties, and reactions of DNA, in: DNA Structure and Function, Academic Press, 1994, pp. 1–57.
[47] P. Catasti, G. Gupta, A.E. Garcia, R. Ratliff, L. Hong, P. Yau, R.K. Moyzis, E. M. Bradbury, Unusual structures of the tandem repetitive DNA sequences located at human centromeres, Biochemistry 33 (1994) 3819–3830, https://doi.org/10.1021/bi00179a005.
[48] J.A.H. Cognet, J. Gabarro-Arpa, M. Le Bret, G.A. van der Marel, J.H. van Boom, G. V. Fazakerley, Solution conformation of an oligonucleotide containing a G.G mismatch determined by nuclear magnetic resonance and molecular mechanics, Nucleic Acids Res. 19 (1991) 6771–6779, https://doi.org/10.1093/nar/19.24.6771.
[49] J.V. Skelly, K.J. Edwards, T.C. Jenkins, S. Neidle, Crystal structure of an oligonucleotide duplex containing G-G base pairs: influence of mispairing on DNA backbone conformation, Proc. Natl. Acad. Sci. USA 90 (1993) 804–808, https://doi.org/10.1073/pnas.90.3.80.
[50] J.-W. Cheng, S.-H. Chou, B.R. Reid, Base pairing geometry in GA mismatches depends entirely on the neighboring sequence, J. Mol. Biol. 228 (1992) 1037–1041, https://doi.org/10.1016/0022-2836(92)90312-8.

[51] H.T. Allawi, J. Santalucia, Nearest neighbor thermodynamic parameters for internal G·a mismatches in DNA, Biochemistry 37 (1998) 2170–2179, https://doi.org/10.1021/bi9724873.

[52] V. Gervais, J.A.H. Cognet, M. Le Bret, L.C. Sowers, G.V. Fazakerley, Solution structure of two mismatches A.A and T.T in the K-ras gene context by nuclear magnetic resonance and molecular dynamics, Eur. J. Biochem. 228 (1995) 279–290, https://doi.org/10.1111/j.1432-1033.1995.0279n.x.

[53] K. Maskos, B.M. Gunn, D.A. LeBlanc, K.M. Morden, NMR study of G·A and A·A pairing in (dGCGAATAAGCG)$_2$, Biochemistry 32 (1993) 3583–3595, https://doi.org/10.1021/bi00065a009.

[54] Y. Lee, S. Gu, H.M. Al-Hashimi, Insights into the A-C mismatch conformational ensemble in duplex DNA and its role in genetic processes through a structure-based review, J. Mol. Biol. 436 (2024) 168710, https://doi.org/10.1016/j.jmb.2024.168710.

[55] X. Gao, D.J. Patel, NMR studies of A-C mismatches in DNA dodecanucleotides at acidic pH, J. Biol. Chem. 262 (1987) 16973–16984, https://doi.org/10.1016/S0021-9258(18)45480-4.

[56] H.T. Allawi, J. Santalucia, Thermodynamics of internal C·T mismatches in DNA, Nucleic Acids Res. 26 (1998) 2694–2701, https://doi.org/10.1093/nar/26.11.2694.

[57] Y. Boulard, J.A.H. Cognet, G.V. Fazakerley, Solution structure as a function of pH of two central mismatches, C-T and C-C, in the 29 to 39 K-ras gene sequence, by nuclear magnetic resonance and molecular dynamics, J. Mol. Biol. 268 (1997) 331–347, https://doi.org/10.1006/jmbi.1997.0975.

[58] L.M. Oliveira, A.S. Long, T. Brown, K.R. Fox, G. Weber, Melting temperature measurement and mesoscopic evaluation of single, double and triple DNA mismatches, Chem. Sci. 11 (2020) 8273–8287, https://doi.org/10.1039/d0sc01700k.

[59] M. Kouchakdjian, B.F.L. Li, P.F. Swann, D.J. Patel, Pyrimidine l pyrimidine base-pair mismatches in DNA - a nuclear magnetic resonance study of T - T pairing at neutral pH and C - C pairing at acidic pH in dodecanucleotide duplexes, J. Mol. Biol. 202 (1988) 139–155, https://doi.org/10.1016/0022-2836(88)90526-8.

[60] M. Peyrard, A.R. Bishop, Statistical mechanics of a nonlinear model for DNA denaturation, Phys. Rev. Lett. 62 (1989) 2755–2758, https://doi.org/10.1103/PhysRevLett.62.2755.

[61] A. Afek, H. Shi, A. Rangadurai, H. Sahay, A. Senitzki, S. Xhani, M. Fang, R. Salinas, Z. Mielko, M.A. Pufall, G.M.K. Poon, T.E. Haran, M.A. Schumacher, H. M. Al-Hashimi, R. Gordân, DNA mismatches reveal conformational penalties in protein–DNA recognition, Nature 587 (2020) 291–296, https://doi.org/10.1038/s41586-020-2843-2.

[62] G. Obmolova, C. Ban, P. Hsieh, W. Yang, Crystal structures of mismatch repair protein MutS and its complex with a substrate DNA, Nature 407 (2000) 703–710, https://doi.org/10.1038/35037509.

[63] M. Sharma, A.V. Predeus, S. Mukherjee, M. Feig, DNA bending propensity in the presence of base mismatches: implications for DNA repair, J. Phys. Chem. B 117 (2013) 6194–6205, https://doi.org/10.1021/jp403127a.

[64] A. Kingsland, L. Maibaum, DNA Base pair mismatches induce structural changes and alter the free-energy landscape of base Flip, J. Phys. Chem. B 122 (2018) 12251–12259, https://doi.org/10.1021/acs.jpcb.8b06007.

[65] G. Rossetti, P.D. Dans, I. Gomez-Pinto, I. Ivani, C. Gonzalez, M. Orozco, The structural impact of DNA mismatches, Nucleic Acids Res. 43 (2015) 4309–4321, https://doi.org/10.1093/nar/gkv254.

[66] J. Brown, T. Brown, K.R. Fox, Affinity of mismatch-binding protein MutS for heteroduplexes containing different mismatches, Biochem. J. 354 (2001) 627–633, https://doi.org/10.1042/bj3540627.

[67] R.J. Isaacs, H.P. Spielmann, A model for initial DNA lesion recognition by NER and MMR based on local conformational flexibility, DNA Repair (Amst) 3 (2004) 455–464, https://doi.org/10.1016/j.dnarep.2004.01.004.

[68] H. Wang, Y. Yang, M.J. Schofield, C. Du, Y. Fridman, S.D. Lee, E.D. Larson, J. T. Drummond, E. Alani, P. Hsieh, D.A. Erie, DNA bending and unbending by MutS govern mismatch recognition and specificity, Proc. Natl. Acad. Sci. 100 (2003) 14822–14827, https://doi.org/10.1073/pnas.2433654100.

[69] S.J. Johnson, L.S. Beese, Structures of mismatch replication errors observed in a DNA polymerase, Cell 116 (2004) 803–816, https://doi.org/10.1016/S0092-8674(04)00252-1.

[70] A. Granzhan, N. Kotera, M.-P. Teulade-Fichou, Finding needles in a basestack: recognition of mismatched base pairs in DNA by small molecules, Chem. Soc. Rev. 43 (2014) 3630–3665, https://doi.org/10.1039/C3CS60455A.

[71] A. Granzhan, E. Largy, N. Saettel, M.P. Teulade-Fichou, Macrocyclic DNA-mismatch-binding ligands: structural determinants of selectivity, Chem. Eur. J. 16 (2010) 878–889, https://doi.org/10.1002/CHEM.200901989.

[72] N. Berthet, J. Michon, J. Lhomme, M.-P. Teulade-Fichou, J.P. Vigneron, J.-M. Lehn, Recognition of abasic sites in DNA by a cyclobisacridine molecule, Chem. Eur. J. 5 (1999) 3625–3630, https://doi.org/10.1002/(SICI)1521-3765(19991203)5:12<3625::AID-CHEM3625>3.0.CO;2-G.

[73] M. Bahr, V. Rie Gabelica, A. Granzhan, M.-P. Teulade-Fichou, E. Weinhold, Selective recognition of pyrimidine-pyrimidine DNA mismatches by distance-constrained macrocyclic bis-intercalators, Nucleic Acids Res. 36 (2008) 5000–5012, https://doi.org/10.1093/nar/gkn392.

[74] K. Nakatani, S. Sando, H. Kumasawa, J. Kikuchi, I. Saito, Recognition of guanine-guanine mismatches by the dimeric form of 2-amino-1,8-naphthyridine, J. Am. Chem. Soc. 123 (2001) 12650–12657, https://doi.org/10.1021/ja0109186.

[75] S. Hagihara, K. Nakatani, I. Saito, Recognition of DNA mismatch structures, Nucleic Acids Res. Suppl. 2 (2002) 127–128, https://doi.org/10.1093/nass/2.1.127.

[76] R. Satange, A.B. Rode, M.-H. Hou, Revisiting recent unusual drug-DNA complex structures: implications for cancer and neurological disease diagnostics and therapeutics, Bioorg. Med. Chem. 76 (2022) 117094, https://doi.org/10.1016/j.bmc.2022.117094.

[77] P.-C. Wu, S.-L. Tzeng, C. Chang, Y.-F. Kao, M.J. Waring, M.-H. Hou, Cooperative recognition of T:T mismatch by echinomycin causes structural distortions in DNA duplex, Nucleic Acids Res. 46 (2018) 7396–7404, https://doi.org/10.1093/nar/gky345.

[78] R. Satange, C.-C. Chang, L. Li, S.-H. Lin, S. Neidle, M.-H. Hou, Synergistic binding of actinomycin D and echinomycin to DNA mismatch sites and their combined anti-tumour effects, Nucleic Acids Res. 51 (2023) 3540–3555, https://doi.org/10.1093/nar/gkad156.

[79] B.A. Jackson, J.K. Barton, Recognition of DNA Base mismatches by a rhodium intercalator, J. Am. Chem. Soc. 119 (1997) 12986–12987, https://doi.org/10.1021/ja972489a.

[80] B.A. Jackson, V.Y. Alekseyev, J.K. Barton, A versatile mismatch recognition agent: specific cleavage of a plasmid DNA at a single base mispair, Biochemistry 38 (1999) 4655–4662, https://doi.org/10.1021/bi990255t.

[81] J.L. Kisko, J.K. Barton, Recognition of DNA base pair mismatches by a cyclometalated Rh(III) intercalator, Inorg. Chem. 39 (2000) 4942–4949, https://doi.org/10.1021/ic000549z.

[82] H. Junicke, J.R. Hart, J. Kisko, O. Glebov, I.R. Kirsch, J.K. Barton, A rhodium(III) complex for high-affinity DNA base-pair mismatch recognition, Proc. Natl. Acad. Sci. USA 100 (2003) 3737–3742, https://doi.org/10.1073/PNAS.0537194100.

[83] J.R. Hart, O. Glebov, R.J. Ernst, I.R. Kirsch, J.K. Barton, DNA mismatch-specific targeting and hypersensitivity of mismatch-repair-deficient cells to bulky rhodium(III) intercalators, Proc. Natl. Acad. Sci. USA 103 (2006) 15359–15363, https://doi.org/10.1073/PNAS.0607576103.

[84] R.J. Ernst, A.C. Komor, J.K. Barton, Selective cytotoxicity of rhodium metalloinsertors in mismatch repair-deficient cells, Biochemistry 50 (2011) 10919–10928, https://doi.org/10.1021/bi2015822.

[85] J.M. Bailis, A.G. Weidmann, N.F. Mariano, J.K. Barton, Rhodium metalloinsertor binding generates a lesion with selective cytotoxicity for mismatch repair-deficient cells, Proc. Natl. Acad. Sci. USA 114 (2017) 6948–6953, https://doi.org/10.1073/pnas.1706665114.

[86] K.M. Boyle, A. Nano, C. Day, J.K. Barton, Cellular target of a rhodium metalloinsertor is the DNA base pair mismatch, Chem. Eur. J. 25 (2019) 3014–3019, https://doi.org/10.1002/chem.201900042.

[87] A. Nano, A.N. Boynton, J.K. Barton, A rhodium-cyanine fluorescent probe: detection and signaling of mismatches in DNA, J. Am. Chem. Soc. 139 (2017) 17301–17304, https://doi.org/10.1021/jacs.7b10639.

[88] A.C. Komor, C.J. Schneider, A.G. Weidmann, J.K. Barton, Cell-selective biological activity of rhodium metalloinsertors correlates with subcellular localization, J. Am. Chem. Soc. 134 (2012) 19223–19233, https://doi.org/10.1021/ja3090687.

[89] A. Nano, J.M. Bailis, N.F. Mariano, E.D. Pham, S.D. Threatt, J.K. Barton, Cell-selective cytotoxicity of a fluorescent rhodium metalloinsertor conjugate results from irreversible DNA damage at base pair mismatches, Biochemistry 59 (2020) 717–726, https://doi.org/10.1021/acs.biochem.9b01037.

[90] A.G. Weidmann, A.C. Komor, J.K. Barton, Biological effects of simple changes in functionality on rhodium metalloinsertors, Philos. Transact. R. Soc. A 371 (2013) 20120117, https://doi.org/10.1098/rsta.2012.0117.

[91] J.K. Barton, A.N. Boynton, K.M. Boyle, Targeting DNA mismatches with coordination complexes, in: M.J. Waring (Ed.), DNA-Targeting Molecules as Therapeutic Agents, Royal Society of Chemistry, 2018, pp. 367–390, https://doi.org/10.1039/9781788012928-fp001.

[92] M.R. Gill, J.A. Thomas, Ruthenium(II) polypyridyl complexes and DNA - from structural probes to cellular imaging and therapeutics, Chem. Soc. Rev. 41 (2012) 3179–3192, https://doi.org/10.1039/C2CS15299A.

[93] M.R. Gill, S.N. Harun, S. Halder, R.A. Boghozian, K. Ramadan, H. Ahmad, K. A. Vallis, A ruthenium polypyridyl intercalator stalls DNA replication forks, radiosensitizes human cancer cells and is enhanced by Chk1 inhibition, Sci. Rep. 6 (2016) 31973, https://doi.org/10.1038/srep31973.

[94] M.R. Gill, P.J. Jarman, S. Halder, M.G. Walker, H.K. Saeed, J.A. Thomas, C. Smythe, K. Ramadan, K.A. Vallis, A three-in-one-bullet for oesophageal cancer: replication fork collapse, spindle attachment failure and enhanced radiosensitivity generated by a ruthenium(ii) metallo-intercalator, Chem. Sci. 9 (2018) 841–849, https://doi.org/10.1039/c7sc03712k.

[95] M.R. Gill, H. Derrat, C. Smythe, G. Battaglia, J.A. Thomas, Ruthenium(II) metallo-intercalators: DNA imaging and cytotoxicity, ChemBioChem 12 (2011) 877–880, https://doi.org/10.1002/cbic.201000782.

[96] A.E. Friedman, J.-C. Chambron, J.-P. Sauvage, N.J. Turro, J.K. Barton, Molecular "light switch" for DNA Ru(bpy)$_2$(dppz)$^{2+}$, J. Am. Chem. Soc. 112 (1990) 4960–4962, https://doi.org/10.1021/ja00168a052.

[97] J. SantaLucia, D. Hicks, The thermodynamics of DNA structural motifs, Annu. Rev. Biophys. Biomol. Struct. 33 (2004) 415–440, https://doi.org/10.1146/annurev.biophys.32.110601.141800.

[98] M.H. Lim, H. Song, E.D. Olmon, E.E. Dervan, J.K. Barton, Sensitivity of Ru(bpy)$_2$dppz^{2+} luminescence to DNA defects, Inorg. Chem. 48 (2009) 5392–5397, https://doi.org/10.1021/ic900407n.

[99] H. Song, J.T. Kaiser, J.K. Barton, Crystal structure of Δ-[Ru(bpy)$_2$dppz]$^{2+}$ bound to mismatched DNA reveals side-by-side metalloinsertion and intercalation, Nat. Chem. 4 (2012) 615–620, https://doi.org/10.1038/nchem.1375.

[100] E. Rüba, J.R. Hart, J.K. Barton, [Ru(bpy)$_2$(L)]Cl$_2$: luminescent metal complexes that bind DNA base mismatches, Inorg. Chem. 43 (2004) 4570–4578, https://doi.org/10.1021/ic0499291.

[101] A.J. McConnell, M.H. Lim, E.D. Olmon, H. Song, E.E. Dervan, J.K. Barton, Luminescent properties of ruthenium(II) complexes with sterically expansive ligands bound to DNA defects, Inorg. Chem. 51 (2012) 12511–12520, https://doi.org/10.1021/ic3019524.
[102] T. Nandhini, K.R. Anju, V.M. Manikandamathavan, V.G. Vaidyanathan, B.U. Nair, Interactions of Ru(II) polypyridyl complexes with DNA mismatches and abasic sites, Dalton Trans. 44 (2015) 9044–9051, https://doi.org/10.1039/c5dt00807g.
[103] A.N. Boynton, L. Marcélis, J.K. Barton, $[Ru(Me_4phen)_2dppz]^{2+}$, a light switch for DNA mismatches, J. Am. Chem. Soc. 138 (2016) 5020–5023, https://doi.org/10.1021/jacs.6b02022.
[104] A.N. Boynton, L. Marcélis, A.J. McConnell, J.K. Barton, A ruthenium(II) complex as a luminescent probe for DNA mismatches and abasic sites, Inorg. Chem. 56 (2017) 8381–8389, https://doi.org/10.1021/acs.inorgchem.7b01037.
[105] Q. Deraedt, L. Marcélis, F. Loiseau, B. Elias, Towards mismatched DNA photoprobes and photoreagents: "elbow-shaped" Ru(II) complexes, Inorg. Chem. Front. 4 (2017) 91–103, https://doi.org/10.1039/c6qi00223d.
[106] M. Gillard, B. Laramée-Milette, Q. Deraedt, G.S. Hanan, F. Loiseau, J. Dejeu, E. Defrancq, B. Elias, L. Marcélis, Photodetection of DNA mismatches by dissymmetric Ru(II) acridine based complexes, Inorg. Chem. Front. 6 (2019) 2260–2270, https://doi.org/10.1039/c9qi00133f.
[107] C.J. Cardin, J.M. Kelly, S.J. Quinn, Photochemically active DNA-intercalating ruthenium and related complexes-insights by combining crystallography and transient spectroscopy, Chem. Sci. 8 (2017) 4705–4723, https://doi.org/10.1039/c7sc01070b.
[108] J.P. Hall, P.M. Keane, H. Beer, K. Buchner, G. Winter, T.L. Sorensen, D.J. Cardin, J.A. Brazier, C.J. Cardin, Delta chirality ruthenium "light-switch" complexes can bind in the minor groove of DNA with five different binding modes, Nucleic Acids Res. 44 (2016) 9472–9482, https://doi.org/10.1093/nar/gkw753.
[109] H. Niyazi, J.P. Hall, K. O'Sullivan, G. Winter, T. Sorensen, J.M. Kelly, C.J. Cardin, Crystal structures of λ-$[Ru(phen)_2dppz]^{2+}$ with oligonucleotides containing TA/TA and AT/AT steps show two intercalation modes, Nat. Chem. 4 (2012) 621–628, https://doi.org/10.1038/nchem.1397.
[110] J.P. Hall, K. O'Sullivan, A. Naseer, J.A. Smith, J.M. Kelly, C.J. Cardin, Structure determination of an intercalating ruthenium dipyridophenazine complex which kinks DNA by semiintercalation of a tetraazaphenanthrene ligand, Proc. Natl. Acad. Sci. 108 (2011) 17610–17614, https://doi.org/10.1073/pnas.1108685108.
[111] T.D. Prieto Otoya, K.T. McQuaid, J. Hennessy, G. Menounou, A. Gibney, N. G. Paterson, D.J. Cardin, A. Kellett, C.J. Cardin, Probing a major DNA weakness: resolving the groove and sequence selectivity of the diimine complex Λ-$[Ru(phen)_2phi]^{2+}$, Angew. Chem. Int. Ed. 63 (2024) e202318863 https://doi.org/10.1002/anie.202318863.
[112] T.D. Prieto Otoya, K.T. McQuaid, N.G. Paterson, D.J. Cardin, A. Kellett, C. J. Cardin, Re-pairing DNA: binding of a ruthenium phi complex to a double mismatch, Chem. Sci. 15 (2024) 9096–9103, https://doi.org/10.1039/d4sc01448k.
[113] M.R. Gill, M.G. Walker, S. Able, O. Tietz, A. Lakshminarayanan, R. Anderson, R. Chalk, A.H. El-Sagheer, T. Brown, J.A. Thomas, K.A. Vallis, An ^{111}In-labelled bis-ruthenium(II) dipyridophenazine theranostic complex: mismatch DNA binding and selective radiotoxicity towards MMR-deficient cancer cells, Chem. Sci. 11 (2020) 8936–8944, https://doi.org/10.1039/D0SC02825H.
[114] C.E. Elgar, N.A. Yusoh, P.R. Tiley, N. Kolozsvári, L.G. Bennett, A. Gamble, E. V. Péan, M.L. Davies, C.J. Staples, H. Ahmad, M.R. Gill, Ruthenium(II) polypyridyl complexes as FRET donors: structure- and sequence-selective DNA-binding and anticancer properties, J. Am. Chem. Soc. 145 (2023) 1236–1246, https://doi.org/10.1021/jacs.2c11111.
[115] D. Wang, S.J. Lippard, Cellular processing of platinum anticancer drugs, Nat. Rev. Drug Discov. 4 (2005) 307–320, https://doi.org/10.1038/nrd1691.
[116] A. Kothandapani, A. Sawant, V.S.M.N. Dangeti, R.W. Sobol, S.M. Patrick, Epistatic role of base excision repair and mismatch repair pathways in mediating cisplatin cytotoxicity, Nucleic Acids Res. 41 (2013) 7332–7343, https://doi.org/10.1093/nar/gkt479.
[117] A. Sawant, A. Kothandapani, A. Zhitkovich, R.W. Sobol, S.M. Patrick, Role of mismatch repair proteins in the processing of cisplatin interstrand cross-links, DNA Repair (Amst) 35 (2015) 126–136, https://doi.org/10.1016/j.dnarep.2015.10.003.
[118] R.P. Topping, J.C. Wilkinson, K.D. Scarpinato, Mismatch repair protein deficiency compromises cisplatin-induced apoptotic signaling, J. Biol. Chem. 284 (2009) 14029–14039, https://doi.org/10.1074/jbc.M809303200.
[119] S. Aebi, B. Kurdi-Haidar, R. Gordon, B. Cenni, H. Zheng, D. Fink, R.D. Christen, C. R. Boland, M. Koi, R. Fishel, S.B. Howell, Loss of DNA mismatch repair in acquired resistance to cisplatin, Cancer Res. 56 (1996) 3087–3090.
[120] D. Jaramillo, N.J. Wheate, S.F. Ralph, W.A. Howard, Y. Tor, J.R. Aldrich-Wright, Polyamide platinum anticancer complexes designed to target specific DNA sequences, Inorg. Chem. 45 (2006) 6004–6013, https://doi.org/10.1021/ic060383n.
[121] D.-L. Ma, C.-M. Che, S.-C. Yan, Platinum(II) complexes with dipyridophenazine ligands as human telomerase inhibitors and luminescent probes for G-quadruplex DNA, J. Am. Chem. Soc. 131 (2009) 1835–1846, https://doi.org/10.1021/ja806045x.
[122] J.A.G. Williams, A. Beeby, E.S. Davies, J.A. Weinstein, C. Wilson, An alternative route to highly luminescent platinum(II) complexes: cyclometalation with N^C^N-coordinating dipyridylbenzene ligands, Inorg. Chem. 42 (2003) 8609–8611, https://doi.org/10.1021/ic035083+.
[123] S.K. Fung, T. Zou, B. Cao, T. Chen, W.-P. To, C. Yang, C.-N. Lok, C.-M. Che, Luminescent platinum(II) complexes with functionalized N-heterocyclic carbene or diphosphine selectively probe mismatched and abasic DNA, Nat. Commun. 7 (2016) 10655, https://doi.org/10.1038/ncomms10655.
[124] M.T. Gabr, F.C. Pigge, Platinum(II) complexes with sterically expansive tetraarylethylene ligands as probes for mismatched DNA, Inorg. Chem. 57 (2018) 12641–12649, https://doi.org/10.1021/acs.inorgchem.8b01782.
[125] L.K. McKenzie, H.E. Bryant, J.A. Weinstein, Transition metal complexes as photosensitisers in one- and two-photon photodynamic therapy, Coord. Chem. Rev. 379 (2018) 2–29, https://doi.org/10.1016/j.ccr.2018.03.020.
[126] M.R. Gill, K.A. Vallis, Transition metal compounds as cancer radiosensitizers, Chem. Soc. Rev. 48 (2019) 540–557, https://doi.org/10.1039/C8CS00641E.
[127] N.A. Yusoh, S.W. Leong, S.L. Chia, S.N. Harun, M.B.A. Rahman, K.A. Vallis, M. R. Gill, H. Ahmad, Metallointercalator $[Ru(dppz)_2(PIP)]^{2+}$ renders BRCA wild-type triple-negative breast cancer cells hypersensitive to PARP inhibition, ACS Chem. Biol. 15 (2020) 378–387, https://doi.org/10.1021/acschembio.9b00843.
[128] N.A. Yusoh, S.L. Chia, N. Saad, H. Ahmad, M.R. Gill, Synergy of ruthenium metallo-intercalator, $[Ru(dppz)_2(PIP)]^{2+}$, with PARP inhibitor Olaparib in non-small cell lung cancer cells, Sci. Rep. 13 (2023) 1456, https://doi.org/10.1038/s41598-023-28454-x.
[129] N.A. Yusoh, P.R. Tiley, S.D. James, S.N. Harun, J.A. Thomas, N. Saad, L.-W. Hii, S. L. Chia, M.R. Gill, H. Ahmad, Discovery of ruthenium(II) metallocompound and olaparib synergy for cancer combination therapy, J. Med. Chem. 66 (2023) 6922–6937, https://doi.org/10.1021/acs.jmedchem.3c00322.
[130] R.T. Mertens, S. Gukathasan, A.S. Arojojoye, C. Olelewe, S.G. Awuah, Next generation gold drugs and probes: chemistry and biomedical applications, Chem. Rev. 123 (2023) 6612–6667, https://doi.org/10.1021/acs.chemrev.2c00649.
[131] A. Erxleben, Interactions of copper complexes with nucleic acids, Coord. Chem. Rev. 360 (2018) 92–121, https://doi.org/10.1016/j.ccr.2018.01.008.
[132] G. Barone, A. Terenzi, A. Lauria, A.M. Almerico, J.M. Leal, N. Busto, B. García, DNA-binding of nickel(II), copper(II) and zinc(II) complexes: structure-affinity relationships, Coord. Chem. Rev. 257 (2013) 2848–2862, https://doi.org/10.1016/j.ccr.2013.02.023.
[133] C.A. J. Hooper, L. Cardo, J.S. Craig, L. Melidis, A. Garai, R.T. Egan, V. Sadovnikova, F. Burkert, L. Male, N.J. Hodges, D.F. Browning, R. Rosas, F. Liu, F.V. Rocha, M.A. Lima, S. Liu, D. Bardelang, M.J. Hannon, Rotaxanating Metallo-supramolecular Nano-cylinder Helicates to Switch DNA Junction Binding, J. Am. Chem. Soc. 142 (2020) 20651–20660, https://doi.org/10.1021/jacs.0c07750.
[134] J. Zhu, C.J.E. Haynes, M. Kieffer, J.L. Greenfield, R.D. Greenhalgh, J.R. Nitschke, U.F. Keyser, FeII4L4 tetrahedron binds to nonpaired DNA bases, J. Am. Chem. Soc. 141 (2019) 11358–11362, https://doi.org/10.1021/jacs.9b03566.
[135] S. Pramanik, L. Khamari, S. Nandi, S. Mukherjee, Discriminating single base pair mismatches in DNA using glutathione-templated copper nanoclusters, J. Phys. Chem. C 123 (2019) 29047–29056, https://doi.org/10.1021/acs.jpcc.9b10069.
[136] J.L. Childs-Disney, X. Yang, Q.M.R. Gibaut, Y. Tong, R.T. Batey, M.D. Disney, Targeting RNA structures with small molecules, Nat. Rev. Drug Discov. 21 (2022) 736–762, https://doi.org/10.1038/s41573-022-00521-4.
[137] R. Kierzek, M.E. Burkard, D.H. Turner, Thermodynamics of single mismatches in RNA duplexes, Biochemistry 38 (1999) 14214–14223, https://doi.org/10.1021/bi991186l.
[138] S. Saxena, Z.O. Jónsson, A. Dutta, Small RNAs with imperfect match to endogenous mRNA repress translation: implications for off-target activity of small inhibitory RNA in mammalian cells, J. Biol. Chem. 278 (2003) 44312–44319, https://doi.org/10.1074/jbc.M307089200.
[139] A. Helwak, G. Kudla, T. Dudnakova, D. Tollervey, Mapping the human miRNA interactome by CLASH reveals frequent noncanonical binding, Cell 153 (2013) 654–665, https://doi.org/10.1016/j.cell.2013.03.043.
[140] S.-H. Bae, H.-K. Cheong, J.-H. Lee, C. Cheong, M. Kainosho, B.-S. Choi, Structural features of an influenza virus promoter and their implications for viral RNA synthesis, Proc. Natl. Acad. Sci. 98 (2001) 10602–10607, https://doi.org/10.1073/pnas.191268798.
[141] A.R. Davis, B.M. Znosko, Thermodynamic characterization of single mismatches found in naturally occurring RNA, Biochemistry 46 (2007) 13425–13436, https://doi.org/10.1021/bi701311c.
[142] A. Murata, M. Nakamori, K. Nakatani, Modulating RNA secondary and tertiary structures by mismatch binding ligands, Methods 167 (2019) 78–91, https://doi.org/10.1016/j.ymeth.2019.05.006.